iScience

CellPress
OPEN ACCESS

Article

Stenotrophomonas maltophilia provokes NEU1-mediated release of a flagellin-binding decoy receptor that protects against lethal infection

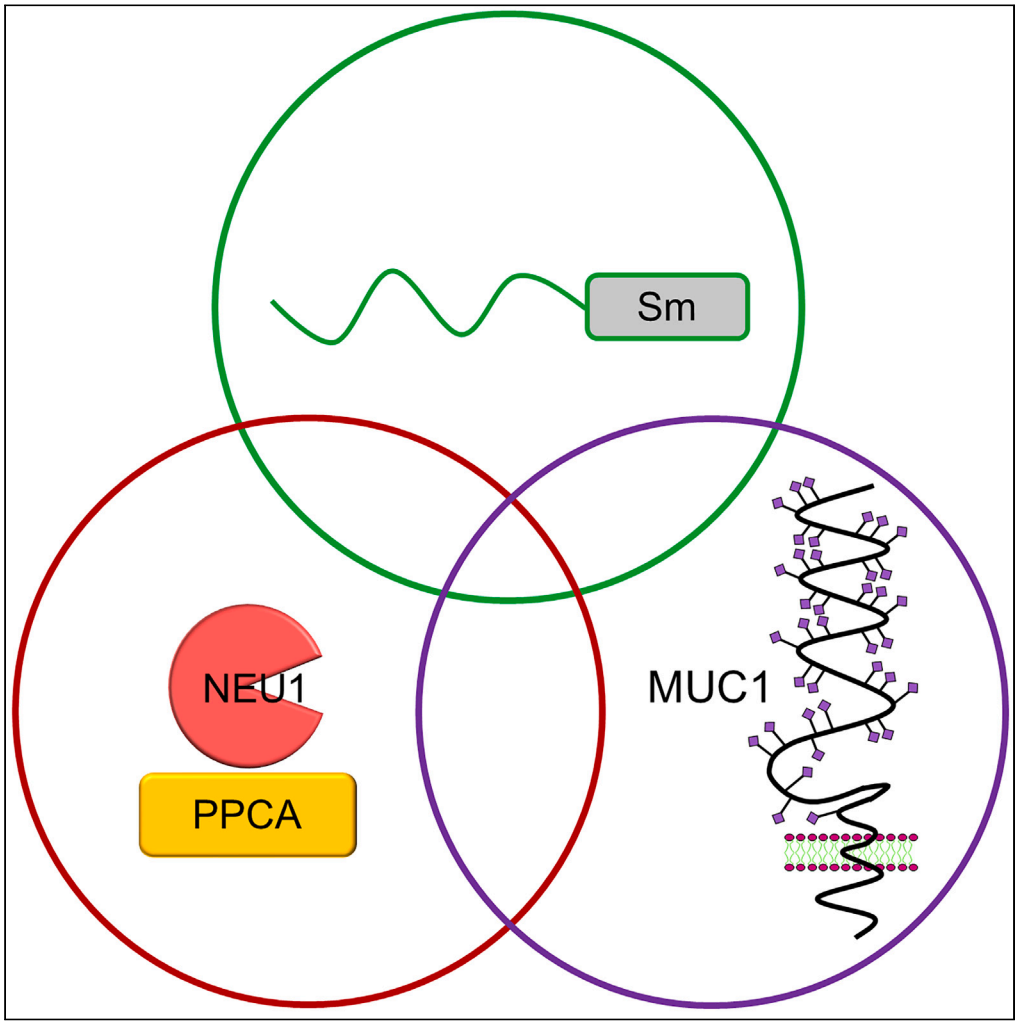

Erik P. Lillehoj, Yafan Yu, Avelino C. Verceles, Akihiro Imamura, Hideharu Ishida, Kurt H. Piepenbrink, Simeon E. Goldblum

elillehoj@gmail.com

Highlights

Sm flagellin binds to the MUC1-ectodomain (ED) on airway epithelial cells

Flagellin-provoked NEU1-mediated MUC1-ED desialylation releases it from cells

The released MUC1-ED decoy receptor disrupts flagellin-driven processes

The MUC1-ED decoy receptor protects against lethal infection

Lillehoj et al., iScience 27, 110866
September 20, 2024
https://doi.org/10.1016/j.isci.2024.110866

iScience

CellPress
OPEN ACCESS

Article

Stenotrophomonas maltophilia provokes NEU1-mediated release of a flagellin-binding decoy receptor that protects against lethal infection

Erik P. Lillehoj,[1,7,*] Yafan Yu,[2] Avelino C. Verceles,[3] Akihiro Imamura,[4] Hideharu Ishida,[4] Kurt H. Piepenbrink,[2,5,6] and Simeon E. Goldblum[3]

SUMMARY

***Stenotrophomonas maltophilia* (Sm), a multidrug-resistant pathogen often isolated from immunocompromised individuals, presents its flagellin to multimeric tandem repeats within the ectodomain of mucin-1 (MUC1-ED), expressed on airway epithelia. Flagellated Sm increases neuraminidase-1 (NEU1) sialidase association with and desialylation of MUC1-ED. This NEU1-mediated MUC1-ED desialylation unmasks cryptic binding sites for Sm flagellin, increasing flagellin and Sm binding to airway epithelia. MUC1 overexpression increases receptor number whereas NEU1 overexpression elevates receptor binding affinity. Silencing of either MUC1 or NEU1 reduces the flagellin-MUC1 interaction. Sm/flagellin provokes MUC1-ED autoproteolysis at a juxtamembranous glycine-serine peptide bond. MUC1-ED shedding from the epithelium not only occurs *in vitro*, but in the bronchoalveolar compartments of Sm/flagellin-challenged mice and patients with ventilator-associated Sm pneumonia. Finally, the soluble flagellin-targeting, MUC1-ED decoy receptor dose-dependently inhibits multiple Sm flagellin-driven pathogenic processes, *in vitro*, including motility, biofilm formation, adhesion, and proinflammatory cytokine production, and protects against lethal Sm lung infection, *in vivo*.**

INTRODUCTION

The first host barrier, with which bacterial pathogens interact in the airways, is the mucus blanket which covers the epithelium.[1,2] The mucus blanket is made up of 2 distinct yet interacting layers, a highly viscous gel layer overlying a periciliary liquid layer. Members of the mucin family comprise the major protein component of mucus, and can be divided into secreted and cell-associated mucins. Of the 5 major mucins that have been detected in the lung, 2 are secreted, MUC5AC and MUC5B, and 3 are cell-tethered, MUC1, MUC4, and MUC16.[2]

MUC1 is comprised of an NH_2-terminal MUC1 ectodomain (MUC1-ED) coupled to a COOH-terminal MUC1 cytoplasmic domain (MUC1-CD).[1,2] The MUC1-ED contains a variable number of highly sialylated 20-amino acid (aa) tandem repeats distal to a juxtamembranous, ~110 aa SEA (sea urchin sperm protein, enterokinase, agrin) domain. The SEA domain contains a G-S-V-V-V consensus sequence that can undergo autoproteolysis with cleavage occurring at the Gly-Ser peptide bond.[3–6] The 2 resultant MUC1 cleavage products noncovalently bind as a heterodimer. The proline-rich MUC1-ED exhibits an extended, rod-like conformation that protrudes higher above the epithelial cell (EC) surface than other membrane-associated proteins.[7] Here, the MUC1-ED is strategically positioned to interact with bacteria in the airway lumen. In fact, multiple bacteria reportedly bind to the MUC1-ED.[8–12] The MUC1-ED is up to 90% carbohydrate, almost entirely through more than 500 predicted O-linked glycosylation sites within the tandem repeats.[13] The relatively short, 72-aa MUC1-CD contains multiple binding sites for cytosolic signaling molecules.[2] How this multifunctional molecule influences the host response to bacteria remains incompletely understood.

Bacterial flagella are comprised of 3 components: (1) a membrane-embedded basal body, (2) the hook, a flexible linker between the membrane complex and the flagellar filament, and (3) the filament itself, composed of thousands of copies of the flagellin monomer.[14] Flagellin proteins are comprised of 4 distinct domains, D0, D1, D2, and D3.[14] The D0 and D1 domains are predominantly α-helical in structure while the D2 and D3 domains contain a mixture of α-helices and β-sheets. The NH_2- and COOH-terminal domains (D0 and D1) are highly conserved, critical for flagellin monomer polymerization, and separated by an intervening hypervariable region (D2 and D3). The flagellar

[1]Department of Pediatrics, University of Maryland School of Medicine, Baltimore, MD, USA
[2]Department of Biochemistry, University of Nebraska, Lincoln, NE, USA
[3]Department of Medicine, University of Maryland School of Medicine, Baltimore, MD, USA
[4]Institute for Glyco-core Research (iGCORE), Gifu University, Gifu, Japan
[5]Department of Food Science and Technology, University of Nebraska, Lincoln, NE, USA
[6]Department of Chemistry, University of Nebraska, Lincoln, NE, USA
[7]Lead contact
*Correspondence: elillehoj@gmail.com
https://doi.org/10.1016/j.isci.2024.110866

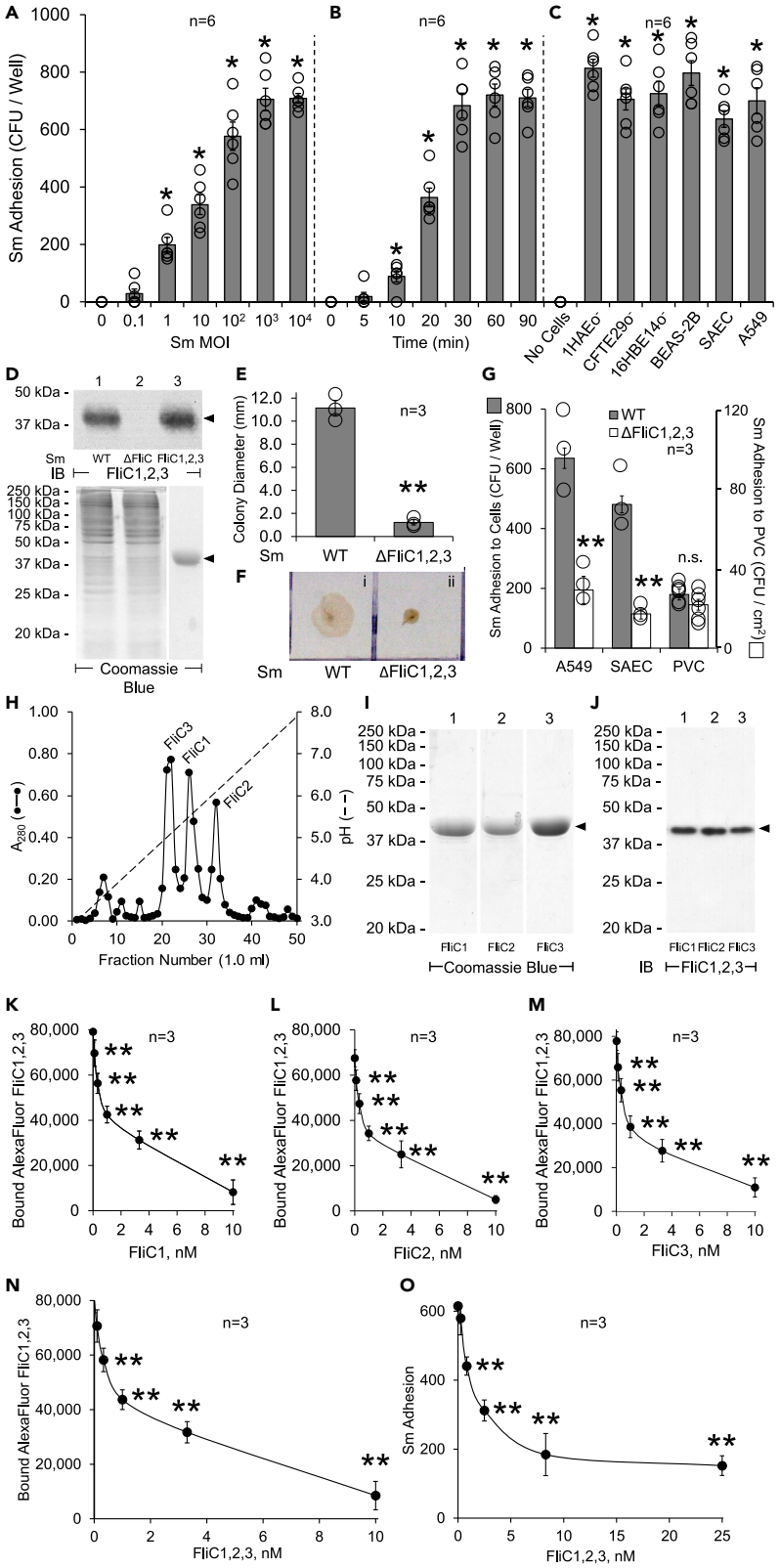
A
B
C
n=6
Sm Adhesion (CFU / Well)
Sm MOI
Time (min)
No Cells
1HAEo-
CFTE29o-
16HBE14o-
BEAS-2B
SAEC
A549
D
Sm
WT
ΔFliC
FliC1,2,3
IB
Coomassie Blue
E
Colony Diameter (mm)
n=3
F
i
ii
G
WT
ΔFliC1,2,3
Sm Adhesion to Cells (CFU / Well)
Sm Adhesion to PVC (CFU / cm²)
n.s.
H
FliC3
FliC1
FliC2
Fraction Number (1.0 ml)
I
J
FliC1
FliC2
FliC3
K
L
M
Bound AlexaFluor FliC1,2,3
FliC1, nM
FliC2, nM
FliC3, nM
N
O
FliC1,2,3, nM
Sm Adhesion

Figure 1. Sm utilizes flagellin to engage human airway epithelia

(A and B) A549 cells were incubated for (A) 30 min with increasing MOIs of Sm or (B) increasing times with Sm at an MOI of 10^3.

(C) 1HAEo$^-$, CFTE29o$^-$, 16HBE14o$^-$, BEAS-2B, SAEC, and A549 cells, or a no cell control were incubated for 30 min with Sm at an MOI of 10^3 and Sm adhesion quantified.

(D) Lysates of flagellin-expressing WT Sm bacteria (lane 1), flagellin-null Sm bacteria (lane 2), and the purified Sm FliC1,2,3 flagellin mixture (lane 3), were resolved by SDS-PAGE and processed for Sm flagellin immunoblotting (IB) and Coomassie blue staining as loading controls for lanes 1 and 2. Bands of interest are indicated by arrowheads on right.

(E) WT and flagellin-null Sm were assayed for motility in colony diameter. Vertical bars represent mean ± SEM colony diameter in mm.

(F) A representative motility plate of WT (panel i) and flagellin-null (panel ii) Sm is shown.

(G) A549 cells, SAECs, and endotracheal tube PVC were incubated with WT or flagellin-null Sm and adherent Sm quantified in CFUs/well (cells) or CFU/cm^2 (PVC).

(A, B, C, G) Vertical bars represent mean ± SEM CFUs/well (cells) or CFU/cm^2 (PVC).

(H) Sm FliC1, FliC2, and FliC3 flagellins were purified by ion-exchange chromatography using a linear pH gradient.

(I) Coomassie blue staining of purified Sm FliC1 (lane 1), FliC2 (lane 2), and FliC3 (lane 3) flagellins.

(J) Flagellin immunoblotting of purified Sm FliC1 (lane 1), FliC2 (lane 2), and FliC3 (lane 3) flagellins.

(K–M) A fixed concentration of the Alexa Fluor 594-conjugated Sm FliC1,2,3 flagellin mixture was incubated with A549 cells in the presence of increasing concentrations of unlabeled FliC1 (K), FliC2 (L), or FliC3 (M) and binding of the labeled flagellins calculated.

(N) A fixed concentration of the Alexa Fluor 594-conjugated Sm FliC1,2,3 flagellin mixture was incubated with A549 cells in the presence of increasing concentrations of unlabeled Sm FliC1,2,3 flagellin mixture and binding of the labeled flagellins calculated.

(O) A fixed inoculum of Sm was co-cultured with A549 cells in the presence of increasing concentrations of the Sm FliC1,2,3 flagellin mixture and Sm adhesion assayed. *, increased Sm adhesion (A-C) compared to the PBS or no cell controls at $p < 0.05$. **, decreased Sm ΔFliC1,2,3 motility (E), adhesion (G, O), or fluoroprobe-labeled FliC1,2,3 flagellin mixture binding (K-N) compared to WT Sm motility, adhesion, or absence of unlabeled flagellin mixture, at $p < 0.05$. n.s., not significant. Statistical comparisons were made using the Student's t test. The results are representative of 3 or 6 independent experiments.

filament participates in bacterial motility, including swimming in liquids and swarming on semi-solid surfaces, adhesion to host proteins, including mucins, and biofilm formation.[14–18] The flagellin monomer is an immunomodulatory agent that has been introduced as an adjuvant for vaccines and assorted immunotherapies.[19]

Stenotrophomonas maltophilia (Sm) expresses 3 flagellin genes, FliC1, FliC2, and FliC3 that form an operon in the Sm genome.[20] The Sm FliC1, FliC2, and FliC3 flagellins self-associate into polar flagella. Sm can be uniflagellated, biflagellated, or multiflagellated. When each flagellin gene is deleted individually or in combination, and the resultant bacteria screened morphologically and functionally, subtle differences can be demonstrated in swimming, swarming, adhesion, and biofilm formation.[20] FliC1, FliC2, and FliC3 contain 406, 400, and 406 aa, respectively. At the aa level, FliC1 shares 67% identity and 76% homology with both FliC2 and FliC3, while FliC2 and FliC3 share 82% identity and 86% homology.[20] Based on their aa sequences, the predicted MWs of FliC1, FliC2, and FliC3 are 41.5 kDa, 40.8 kDa, and 41.4 kDa, respectively (https://www.expasy.org/resources/protparam).

We recently found that *Pseudomonas aeruginosa* (Pa)-expressed flagellin engages the MUC1-ED on the surface of airway epithelia.[21–23] Pa expresses a noncanonical neuraminidase/sialidase (NEU) which contains an active site that does not accommodate sialic acid and lacks sialidase activity.[24] The MUC1-ED-Pa flagellin receptor-ligand interaction recruits the eukaryotic NEU1, together with its chaperone protein, protective protein/cathepsin A (PPCA), to surface-expressed MUC1. PPCA is absolutely required for proper folding, stability, oligomerization, and activation of NEU1.[25] Although NEU1 has been historically studied in context of its indispensable role in glycan catabolism and the lysosomal storage disease, sialidosis,[25–27] it has been detected on the surface of multiple cell types,[28,29] where it desialylates numerous sialoproteins, including MUC1.[21,30] NEU1 desialylation of the MUC1-ED unmasks cryptic binding sites for Pa-derived flagellin, dramatically enhancing Pa adhesion to MUC1-expressing epithelia. At the same time, NEU1-mediated MUC1-ED desialylation permits shedding of the still hyperadhesive, flagellin-targeting MUC1-ED, as a decoy receptor, with both anti-bacterial and anti-inflammatory properties.[21–23] In the current studies, we asked whether this flagellin-provoked, NEU1-mediated generation of the MUC1-ED decoy receptor could be extended to another flagellated, NEU-deficient bacterium, Sm. This multidrug-resistant (MDR) gram-negative, obligate aerobic bacterium is commonly found in the airways of immunocompromised hosts, individuals with cystic fibrosis, and hospitalized patients with ventilator-associated pneumonia.[31] Sm adhesion to endotracheal tubes and subsequent biofilm formation is a major factor contributing to the development of ventilator-associated Sm pneumonia.[32] Sm and Pa can often (1) present in similar patients as the same clinical syndromes, ((2) are cultured from the same environmental sources, (3) can be diagnostically confused in the clinical microbiology laboratory, and (4) are identified as MDR microorganisms.[31–36] In fact, prior to DNA sequencing studies, Pa and Sm were so closely related that Sm was known as *Pseudomonas maltophilia*.[32]

RESULTS

Sm flagellin engages the human airway epithelium

Adhesion of Sm strain KJ bacteria to A549 cells increased as the inoculum size was increased from multiplicities of infection (MOI)s of 1.0–10^3 (Figure 1A). At MOI >10^3, no further increments in Sm adhesion were detected, indicating a finite saturable number of Sm binding sites on these cells. Using a fixed Sm inoculum size (MOI = 10^3), as Sm-A549 cell co-culture times were extended from 10 to 30 min, Sm adhesion increased (Figure 1B). We then incubated Sm (MOI = 10^3) for 30 min with human airway epithelia derived from anatomical sites along the entire length of the airway. ECs derived from the human trachea (1HAEo$^-$ and CFTE29o$^-$ cells), bronchus (16HBE14o$^-$ and BEAS-2B cells), small airways (SAEC), and alveoli (A549 cells) each displayed comparable adhesiveness for Sm (Figure 1C).

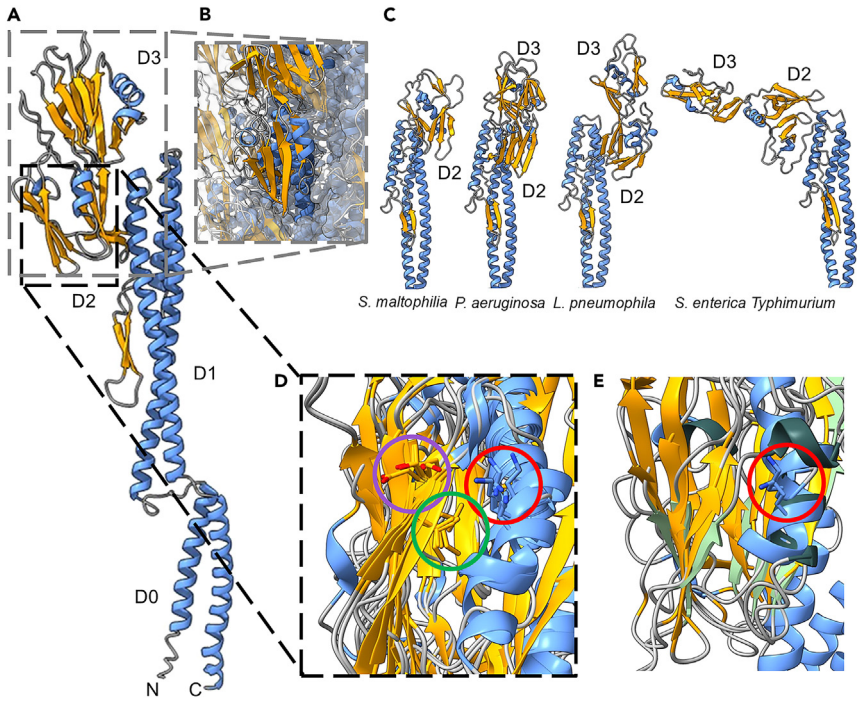

Figure 2. Structural comparison of the flagellin proteins of Sm, Pa, Lp, and STm

(A) X-ray crystallographic structure of Pa FlaB flagellin illustrating the D0, D1, D2, and D3 domains with α-helices shown as blue coils, β-sheets as orange arrows, and loops as gray lines.

(B) Cryo-EM structure of the Pa FlaB flagellar filament illustrating the exposed β-sheets of the D2 (lower) and D3 (upper) domains.

(C) Structures of Sm, Pa, Lp, and STm flagellins. Note the absence of the D3 domain in the Sm flagellins and distinct orientation of the D2 and D3 domains of STm flagellin.

(D) Expanded view of superimposed D2 domains of Sm FliC1, FliC2, and FliC3, and Pa FlaA flagellins. Conserved aa's Val-206 (green circle), Asp-207 (purple circle), and Lys-220 (red circle) (FlaA numbering) are depicted atomistically. Equivalent residues include Val-247, Asn-248, and Lys-258 in Sm FliC1, Val-250, Asp-251, and Lys-263 in Sm FliC2, Val-250, Asp-251, and Lys-264 in Sm FliC3, and Ile-210, Ala-211, and Lys-224 in Pa FlaB.

(E) Expanded view of D2 domains of Sm FliC1 and Pa FlaB flagellins (blue and orange) superimposed with Lp flagellin (green). Lys-258 (Sm FliC1) and Lys-224 (FlaB) are depicted atomistically (red circle).

We next compared flagellin expression in bacterial cell extracts of the wild-type (WT) Sm KJ strain (Figure 1D, lane 1) with that of a flagellin-null strain, Sm ΔFliC1,2,3,[20] in which the 3 flagellin genes had been deleted from the parental KJ strain (Figure 1D, lane 2). Since the 3 Sm flagellin proteins share a high level of aa sequence similarity, are of comparable MWs, and their respective deletion mutants display only subtle functional differences,[20] for selected experiments, we purified a mixture of the 3 flagellins, as well as the individual FliC1, FliC2, and FliC3 proteins, from the WT Sm KJ strain. The purified Sm flagellin preparation containing a mixture of the 3 flagellin proteins, designated as FliC1,2,3, was used as a positive gel-mobility control (Figure 1D, lane 3). When lysates of the flagellin-expressing WT Sm bacterial strain, the flagellin-null Sm strain, and the purified Sm FliC1,2,3 flagellin mixture were resolved and probed with an antibody (Ab) raised against WT Sm flagellin, flagellins were detected in the WT Sm strain (Figure 1D, lane 1) and the flagellin mixture control (Figure 1D, lane 3), but not in flagellin-null Sm (Figure 1D, lane 2). The combined purified FliC1,2,3 flagellin mixture migrated with the same mobility as the Sm-associated flagellins in a whole cell bacterial extract, and each preparation was recognized by the same anti-flagellin Ab as an apparent single protein band with an MW of ~41.0 kDa (Figure 1D, lanes 1, 3). Uncropped immunoblots corresponding to Figure 1D are shown in Figure S1. To functionally evaluate the flagellin-expressing WT and flagellin-null Sm strains, both were assayed for motility (Figures 1E and 1F). The flagellin-null mutant displayed an 89.0% decrease in motility compared to WT Sm. We then asked whether Sm adhesion to human airway ECs and/or endotracheal tube polyvinyl chloride (PVC) was mediated through Sm flagellin expression. Flagellin-null Sm adhesion to A549 cells and SAECs was decreased by 68.0% and 77.1%, respectively, compared to the adhesion of WT Sm to these same cells (Figure 1G). In contrast, adhesion of WT Sm to the PVC substrate was not different than adhesion of flagellin-null Sm (Figure 1G).

To further explore the role of the 3 Sm flagellins, FliC1, FliC2, and FliC3, in bacterial adhesion to airway ECs, we purified the individual proteins from Sm strain KJ bacteria by ion-exchange chromatography (Figure 1H). Each purified flagellin was presumptively identified by its relative elution position compared to its predicted isoelectric point, pI = 5.44 (FliC1), pI = 6.01 (FliC2), and pI = 5.16 (FliC3) (https://web.expasy.org/compute_pi/). The 3 purified flagellins were processed by sodium dodecyl sulfate-polyacrylamide gel electrophoresis (SDS-PAGE) for both Coomassie blue staining (Figure 1I) and flagellin immunoblotting (Figure 1J). Each of the 3 flagellin proteins was recognized by the anti-flagellin Ab and migrated with comparable gel mobilities of ~41.0 kDa. We then asked whether the individual FliC1, FliC2,

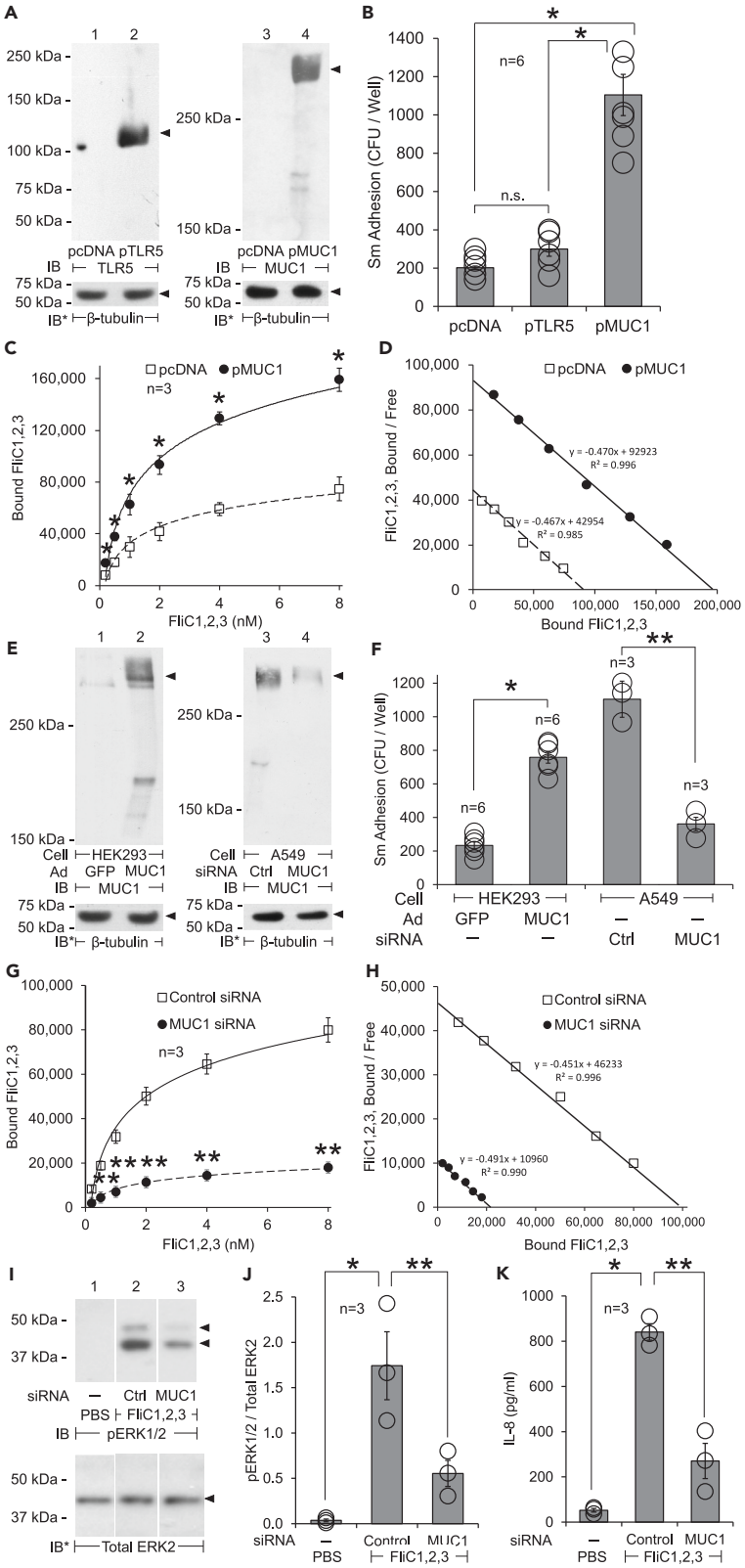
A
1
2
3
4
250 kDa
150 kDa
100 kDa
75 kDa
50 kDa
pcDNA pTLR5
IB TLR5
pcDNA pMUC1
IB MUC1
IB* β-tubulin
B
Sm Adhesion (CFU / Well)
n=6
n.s.
pcDNA
pTLR5
pMUC1
C
pcDNA
pMUC1
n=3
Bound FliC1,2,3
FliC1,2,3 (nM)
D
pcDNA
pMUC1
FliC1,2,3, Bound / Free
Bound FliC1,2,3
y = -0.470x + 92923
R² = 0.996
y = -0.467x + 42954
R² = 0.985
E
Cell HEK293
Ad GFP MUC1
IB MUC1
Cell A549
siRNA Ctrl MUC1
IB* β-tubulin
F
Sm Adhesion (CFU / Well)
n=6
n=3
Cell HEK293 A549
Ad GFP MUC1 — —
siRNA — — Ctrl MUC1
G
Control siRNA
MUC1 siRNA
n=3
Bound FliC1,2,3
FliC1,2,3 (nM)
H
Control siRNA
MUC1 siRNA
FliC1,2,3, Bound / Free
Bound FliC1,2,3
y = -0.451x + 46233
R² = 0.996
y = -0.491x + 10960
R² = 0.990
I
50 kDa
37 kDa
siRNA — Ctrl MUC1
PBS FliC1,2,3
IB pERK1/2
IB* Total ERK2
J
n=3
pERK1/2 / Total ERK2
siRNA — Control MUC1
PBS FliC1,2,3
K
n=3
IL-8 (pg/ml)
siRNA — Control MUC1
PBS FliC1,2,3

Figure 3. Sm flagellin binds to the MUC1-ED

(A) HEK293T cells were transfected with the pcDNA3.1 empty vector, or plasmids encoding for TLR5 (pTLR5) or MUC1 (pMUC1), the cells were lysed and the lysates processed for TLR5 (lanes 1, 2) or MUC1 (lanes 3, 4) immunoblotting. To control for protein loading and transfer, the blots were stripped and reprobed (IB*) for β-tubulin.

(B) HEK293T cells overexpressing TLR5 or MUC1, or empty vector-transfected cells, were incubated with Sm and adherent bacteria quantified. Vertical bars represent mean ± SEM CFUs/well.

(C) A549 cells were transfected with pcDNA3.1 or pMUC1 and binding of increasing concentrations of the Alexa Fluor 594-labeled Sm FliC1,2,3 flagellin mixture determined. Data points represent mean ± SEM bound flagellin in molecules/EC.

(D) Scatchard analysis of binding data in (C). The linear regression equation and R^2 value are indicated adjacent to each line.

(E and F) HEK293T cells were infected with Ad-GFP or Ad-MUC1, and A549 cells were transfected with MUC1-targeting or control siRNAs, and both cell types were cultured for 48 h. (E) Ad-GFP- and Ad-MUC1-infected cells (lanes 1, 2) and MUC1 siRNA- and control siRNA-transfected cells (lanes 3, 4) were lysed and the lysates processed for MUC1 immunoblotting. (F) Infected or transfected cells were incubated with Sm and cell-bound bacteria quantified. Vertical bars represent mean ± SEM Sm adhesion in CFUs/well.

(G) A549 cells were transfected with MUC1-targeting or control siRNAs, cultured for 48 h, and binding of increasing concentrations of the Alexa Fluor 595-labeled Sm FliC1,2,3 flagellin mixture determined. Data points represents mean ± SEM bound flagellin in molecules/EC.

(H) Scatchard analysis of binding data in (G).

(I–K) A549 cells and A549 cells transfected with MUC1-targeting or control siRNAs were incubated for 48 h and then stimulated for 1 h with 10 ng of the Sm FliC1,2,3 flagellin mixture or PBS. (I) Non-transfected, PBS-treated (lane 1), control siRNA-transfected, flagellin-stimulated (lane 2), and MUC1 siRNA-transfected, flagellin-stimulated (lane 3) cells were lysed, and the lysates processed for pERK1/2 immunoblotting. To control for protein loading and transfer, the blots were stripped and reprobed for total ERK2. The ~44.0 kDa pERK1 (upper) and ~42.0 kDa pERK2 (lower) bands, as well as the total ERK2 band, are indicated by arrowheads on the right. (J) Densitometric analysis of pERK1/2 normalized to total ERK2 displayed in (I). Vertical bars represent mean ± SEM normalized pERK1/2 signal. (K) Supernatants from the cells in (I) were processed for IL-8 levels and normalized to total EC protein. Vertical bars represent mean ± SEM normalized IL-8 concentrations in pg/mg EC protein. *, increased Sm adhesion (B, F), flagellin binding (C), ERK activation (J), or normalized IL-8 release (K) compared to pcDNA3.1, pTLR5, Ad-GFP, control siRNA, or PBS controls at $p < 0.05$. **, decreased Sm adhesion (F), flagellin binding (G), ERK activation (J), or normalized IL-8 release (K) compared to the siRNA controls at $p < 0.05$. n.s., not significant. Statistical comparisons were made using the Student's t test. The results are representative of 3 or 6 independent experiments.

and FliC3 flagellins recognized and bound to the same receptor expressed on human airway epithelia. We tested each of the 3 Sm flagellins for its ability to competitively displace the FliC1,2,3 flagellin mixture labeled with the Alexa Fluor 594 fluoroprobe, from binding sites expressed on airway epithelia (Figures 1K, 1K, and 1M). In the absence of the unlabeled flagellins, the fluoroprobe-labeled FliC1,2,3 flagellin mixture displayed robust binding to airway epithelia. When a fixed concentration of the labeled FliC1,2,3 flagellin mixture was assayed for binding to A549 cells in the presence of increasing concentrations of the unlabeled FliC1, FliC2, or FliC3 flagellins, each of the unlabeled flagellins dose-dependently decreased binding of the labeled FliC1,2,3 flagellin mixture (Figures 1K, 1L, and 1M). These data indicate that each of the 3 Sm-derived flagellins bind to the same receptor. Sm and A549 cells were co-cultured in the presence of increasing concentrations of the unlabeled FliC1,2,3 flagellin mixture to test for its ability to competitively displace a fixed concentration of the fluoroprobe-labeled FliC1,2,3 flagellin mixture from binding sites on airway epithelia (Figure 1N). The unlabeled flagellin mixture dose-dependently decreased binding of the labeled flagellin mixture. We then tested whether increasing concentrations of the unlabeled FliC1,2,3 flagellin mixture could interfere with Sm adhesion to airway epithelia (Figure 1O). As the concentration of the flagellin mixture increased, Sm adhesion decreased. These combined results indicate that the exogenous, purified flagellins bind to and occupy one or more receptor(s) on the ECs, thereby preventing docking of Sm-associated flagellins. Although the introduction of unlabeled flagellins specifically and competitively displaced the labeled FliC1,2,3 flagellin mixture (Figures 1K–1N) and diminished Sm adhesion (Figure 1O), the Sm adhesion curve did not approach 0 CFUs/well on the y axis, raising the possibility that one or more bacterial adhesins other than flagellin, such as fimbriae,[37] might also be operative.

Flagellin structural analyses

On the basis of our previous[22,23] and current studies, we found that select bacterial flagellins (Sm FliC1, FliC2, and FliC3, and Pa FlaA and FlaB) bind to airway epithelia to provoke MUC1-ED shedding, whereas other flagellins (*Legionella pneumophila* [Lp] FliC and *Salmonella enterica* serovar Typhimurium [STm] FliC) do not. To establish a structural basis for this inconsistent flagellin bioactivity, we constructed molecular models of these flagellin proteins. Figure 2A displays the ribbon structure of Pa FlaB. Figure 2B shows the cryo-EM structure of Pa FlaB, demonstrating that the D2 and D3 domains each have an exposed β-sheet (orange arrows). Individual structures of Sm, Pa, Lp, and STm flagellins are shown in Figure 2C. The D2 and D3 domains of STm FliC are highly dissimilar and of different orientation compared to the D2 and D3 domains of the Sm, Pa, and Lp flagellins, which may account for the inability of STm FliC to bind to airway ECs to provoke Sm shedding.[23] Further, while the 3 flagellins of Sm each possess the D2 domain, they lack the D3 domain. Superimposition of the D2 domains of the Sm and Pa flagellins reveals 3 conserved aa residues, which in the case of Pa FlaA include Val-206, Asp-207, and Lys-220, that spatially coalesce in the tertiary structure of the proteins (Figure 2D, green, purple, and red circles). In addition, Sm and Pa flagellins possess a groove between their D2 domain β-sheet and the adjacent α-helix (residues 218–225), with the conserved Lys-220 residue in the α-helix. While Lp flagellin also possesses this groove, it is obstructed by a peptide loop encompassing residues 201–218 and its α-helix lacks the conserved Lys residue (Figure 2E). These features may account for the inability of Lp flagellin to bind to airway ECs and provoke MUC1-ED shedding.[23] Taken together, these results suggest that the 3 conserved aa's and/or the groove in the D2 domain between the β-sheet and α-helix of the Sm and Pa flagellins participate in flagellin binding and bacterial adhesion to airway epithelial binding site(s).

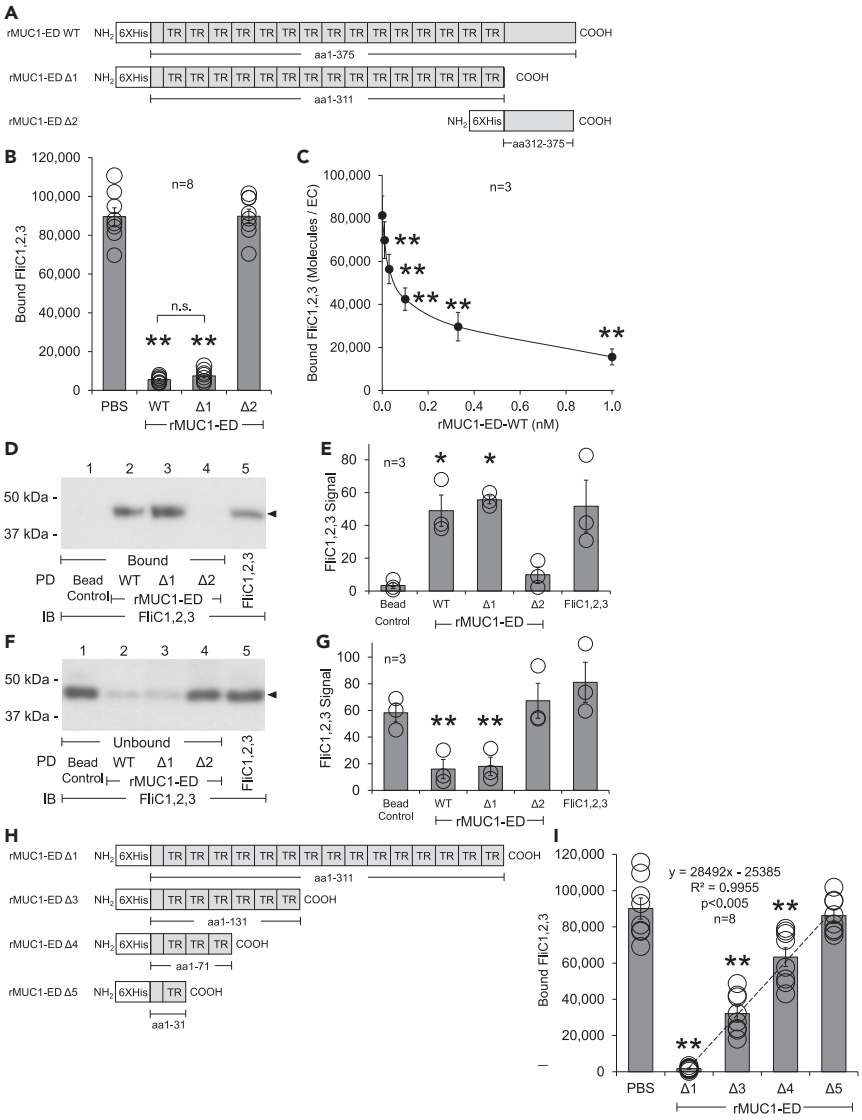

Figure 4. Sm flagellin binds to multimeric tandem repeats within the MUC1-ED

(A) Schematic of rMUC1-ED proteins containing a 6XHis epitope tag fused to each NH_2-terminus, including the (1) rMUC1-ED-WT with 15 tandem repeats, aa 1–375, (2) rMUC1-ED-Δ1 with 15 tandem repeats, aa 1–311, and (3) rMUC1-ED-Δ2 distal to the tandem repeats, aa 312–375. Each 20-aa tandem repeat (G-S-T-A-P-P-A-H-G-V-T-S-A-P-D-T-R-P-A-P) within the MUC1-ED is indicated by TR.

(B) Each recombinant protein displayed in (A) was screened for its ability to inhibit binding of a fixed concentration of the Alexa Fluor 594-conjugated Sm FliC1,2,3 flagellin mixture to MUC1-expressing airway epithelia and bound flagellin in molecules/EC calculated.

(C) A549 cells were incubated with a fixed concentration of Alexa Fluor 594-conjugated Sm FliC1,2,3 flagellin mixture in the presence of increasing concentrations of the rMUC1-ED-WT with 15 tandem repeats and flagellin binding calculated.

(D) The 6XHis-tagged rMUC1-ED proteins in (A) were immobilized on Ni-NTA-agarose beads. The purified Sm FliC1,2,3 flagellin mixture was incubated with the 6XHis-tagged WT-rMUC1-ED, rMUC1-ED-Δ1, or rMUC1-ED-Δ2 proteins immobilized on the beads (lanes 2–4), the Ni-NTA-agarose beads alone (lane 1), or was directly loaded on the gel as a gel mobility control (lane 5). Proteins bound to the beads and the loaded flagellin gel mobility control were processed for flagellin immunoblotting.

(E) Densitometric analysis of flagellin signal in immunoblots displayed in (D).

(F) The proteins unbound to the Ni-NTA-agarose beads in the same samples studied in (D) were processed for flagellin immunoblotting.

(G) Densitometric analysis of flagellin signal in immunoblots displayed in (F). PD, pull-down.

(H) Schematic of rMUC1-ED proteins containing decreasing numbers of tandem repeats and a 6XHis epitope tag fused to each NH_2-terminus, including the (1) rMUC1-ED-Δ1 with 15 tandem repeats, aa 1–311, (2) rMUC1-ED-Δ3 with 6 tandem repeats, aa 1–131, (3) rMUC1-ED-Δ4 with 3 tandem repeats, aa 1–71, and (4) rMUC1-ED-Δ5 with 1 tandem repeat, aa 1–31.

(I) Each recombinant protein displayed in (H) was assayed for its ability to inhibit binding of a fixed concentration of the Alexa Fluor 594-conjugated Sm FliC1,2,3 flagellin mixture to MUC1-expressing airway epithelia and bound flagellin in molecules/EC calculated. The dashed line indicates the linear regression analysis,

Figure 4. *Continued*

and the corresponding linear regression equation and correlation coefficient (R^2) are shown. (B, E, G, and I) Vertical bars represent mean ± SEM FliC1,2,3 flagellin signal. *, increased flagellin signal (E) compared to the bead control at $p < 0.05$. **, decreased bound flagellin (B, C, and I) or flagellin signal (G) compared to the PBS or bead control at $p < 0.05$. n.s., not significant. Statistical comparisons were made using the Student's t test. The results are representative of 3 or 8 independent experiments.

Sm Flagellin binds to the MUC1-ED

Two established receptors for flagellin that are expressed on the surface of airway epithelia include the classical host pattern recognition receptor, Toll-like receptor (TLR)5[38] and MUC1.[39] Given that primary SAECs and A549 cells both co-express MUC1 and TLR5,[2] human embryonic kidney (HEK)293T cells that express extremely low or undetectable endogenous TLR5 and MUC1,[40,41] were transfected for TLR5 expression (Figure 3A, lanes 2 vs. 1) or MUC1 expression (Figure 3A, lane 4 vs. 3). Uncropped immunoblots corresponding to Figure 3A are shown in Figure S2A. First, we compared Sm adhesion to HEK293T cells overexpressing TLR5 to its adhesion to cells transfected with the empty vector control. Robust TLR5 expression did not enhance Sm adhesion (Figure 3B). In contrast, Sm adhesion to HEK293T cells overexpressing MUC1 was increased 5.5-fold compared to cells transfected with the empty vector control and increased 3.8-fold compared to cells overexpressing TLR5 (Figure 3B). To further support a MUC1-flagellin, receptor-ligand interaction, HEK293T cells overexpressing MUC1 or transfected with the empty vector control were incubated with increasing concentrations of the fluoroprobe-labeled FliC1,2,3 flagellin mixture and flagellin binding determined. We found that MUC1 overexpression in HEK293T cells increased the binding of the fluoroprobe-labeled FliC1,2,3 flagellin mixture compared to the empty vector control (Figure 3C). Scatchard analysis of the binding data (Figure 3D) allowed us to quantify the number of flagellin binding sites on the ECs, as indicated by the X axis intercept of the binding plot, and binding affinity of the flagellin-MUC1 interaction, as indicated by the slope of the binding plot ($-1/K_d$), where K_d represents the dissociation constant of the ligand-receptor interaction.[21,22] MUC1 overexpression increased the number of flagellin binding sites 2.1-fold without altering its binding affinity compared to the empty vector control (Figure 3D). While MUC1 overexpression (Figure 3E, lane 2 vs. 1) increased Sm adhesion (Figure 3F), small interfering (si)RNA-induced MUC1 silencing (Figure 3E, lane 4 vs. 3) diminished it (Figure 3F). Uncropped immunoblots corresponding to Figure 3E are shown in Figure S2B. MUC1 knockdown (Figure 3E, lane 4) diminished the number of binding sites for the fluoroprobe-labeled FliC1,2,3 flagellin mixture compared to a nontargeting control siRNA by 78.2% without changing receptor binding affinity (Figures 3G and 3H). Finally, as established biochemical markers of intracellular signaling downstream to the flagellin-MUC1-ED interaction,[42] we assayed for ERK1/2 activation and IL-8 release in airway ECs transfected with MUC1-targeting or nontargeting control siRNAs and stimulated with the Sm FliC1,2,3 flagellin mixture or PBS control (Figures 3I–3K). The FliC1,2,3 flagellin mixture increased ERK1/2 activation by 43.5-fold (Figures 3I and 3J) and IL-8 release by 16.0-fold (Figure 3K), each compared to their respective PBS controls. Prior MUC1 knockdown reduced flagellin-induced ERK1/2 activation by 68.4% (Figure 3J) and diminished IL-8 release by 67.8% (Figure 3K), each compared to their respective siRNA controls. Uncropped, replicate immunoblots corresponding to Figure 3I are shown in Figure S3. These combined data identify MUC1 as the predominant signal-transducing airway epithelial receptor for the Sm-expressed flagellins.

Sm flagellin directly binds to multimeric tandem repeats in the MUC1-ED

We then asked which portion of the MUC1-ED molecule might recognize the Sm-expressed flagellins. First, we screened *Escherichia coli*-expressed recombinant (r)MUC1-ED proteins for their ability to block binding of the Alexa Fluor 488-conjugated FliC1,2,3 flagellin mixture to MUC1-expressing airway epithelia. These rMUC1-ED proteins corresponded to the (1) full-length human rMUC1-ED-WT containing 15 tandem repeats, aa 1–375 (rMUC1-ED-WT), (2) rMUC1-ED NH_2-terminus followed by 15 tandem repeats, aa 1–311 (rMUC1-ED-Δ1), and (3) rMUC1-ED COOH-terminus distal to the tandem repeats, aa 312–375 (rMUC1-ED-Δ2), each containing an NH_2-terminal polyhistidine (6XHis) epitope tag (Figure 4A). The full-length rMUC1-ED-WT and tandem repeat-containing rMUC1-ED-Δ1 deletion mutant each profoundly diminished flagellin binding, whereas equimolar concentrations of the COOH-terminal rMUC1-ED-Δ2 deletion mutant lacking tandem repeats did not (Figure 4B). When increasing concentrations of the full-length rMUC1-ED-WT were tested, it dose-dependently decreased binding of the Alexa Flour 594-labeled Sm FliC1,2,3 flagellin mixture to A549 cells (Figure 4C). To establish a direct Sm flagellin-MUC1-ED interaction in a cell-free system, the FliC1,2,3 flagellin mixture was incubated with each of the 6XHis-tagged rMUC1-ED proteins immobilized on nickel-nitrilotriacetic acid (Ni-NTA)-agarose beads or with the Ni-NTA-agarose beads alone. Proteins bound to the beads and a FliC1,2,3 flagellin mixture gel mobility control were processed for flagellin immunoblotting (Figure 4D and 4E). The flagellin mixture bound to the tandem repeat-containing full-length rMUC1-ED-WT and the rMUC1-ED-Δ1 deletion mutant (Figure 4D, lanes 2, 3), but not to the rMUC1-ED-Δ2 deletion mutant lacking tandem repeats (Figure 4D, lane 4) or the bead control (Figure 4D, lane 1). The proteins that did not bind to Ni-NTA-agarose beads were similarly processed for flagellin immunoblotting as a control (Figures 4F and 4G). The flagellin signal was markedly reduced for those samples incubated with either of the 2 tandem repeat-containing rMUC1-ED proteins (Figure 4F, lanes 2, 3), whereas robust flagellin signal was evident in the sample after incubation with either the rMUC1-Δ2 deletion mutant lacking tandem repeats (Figure 4F, lane 4) or with the beads alone (Figure 4F, lane 1). Uncropped, replicate immunoblots corresponding to Figures 4D and 4F are shown in Figures S4. Finally, to establish the number of tandem repeats required for binding of the Sm FliC1,2,3 flagellin mixture, rMUC1-ED constructs containing 15 tandem repeats, aa 1–311 (rMUC1-ED-Δ1), 6 tandem repeats, aa 1–131 (rMUC1-ED-Δ3), 3 tandem repeats, aa 1–71 (rMUC1-ED-Δ4), or 1 tandem repeat, aa 1–31 (rMUC1-ED-Δ5), each containing an NH_2-terminal 6XHis epitope tag (Figure 4H), were assayed for their ability to inhibit binding of the FliC1,2,3 mixture to A549 cells. First, the rMUC1-ED required ≥ 3 tandem repeats to inhibit binding of Sm flagellin to MUC1-expressing airway epithelia (Figure 4I). Further, rMUC1-ED constructs with increasing

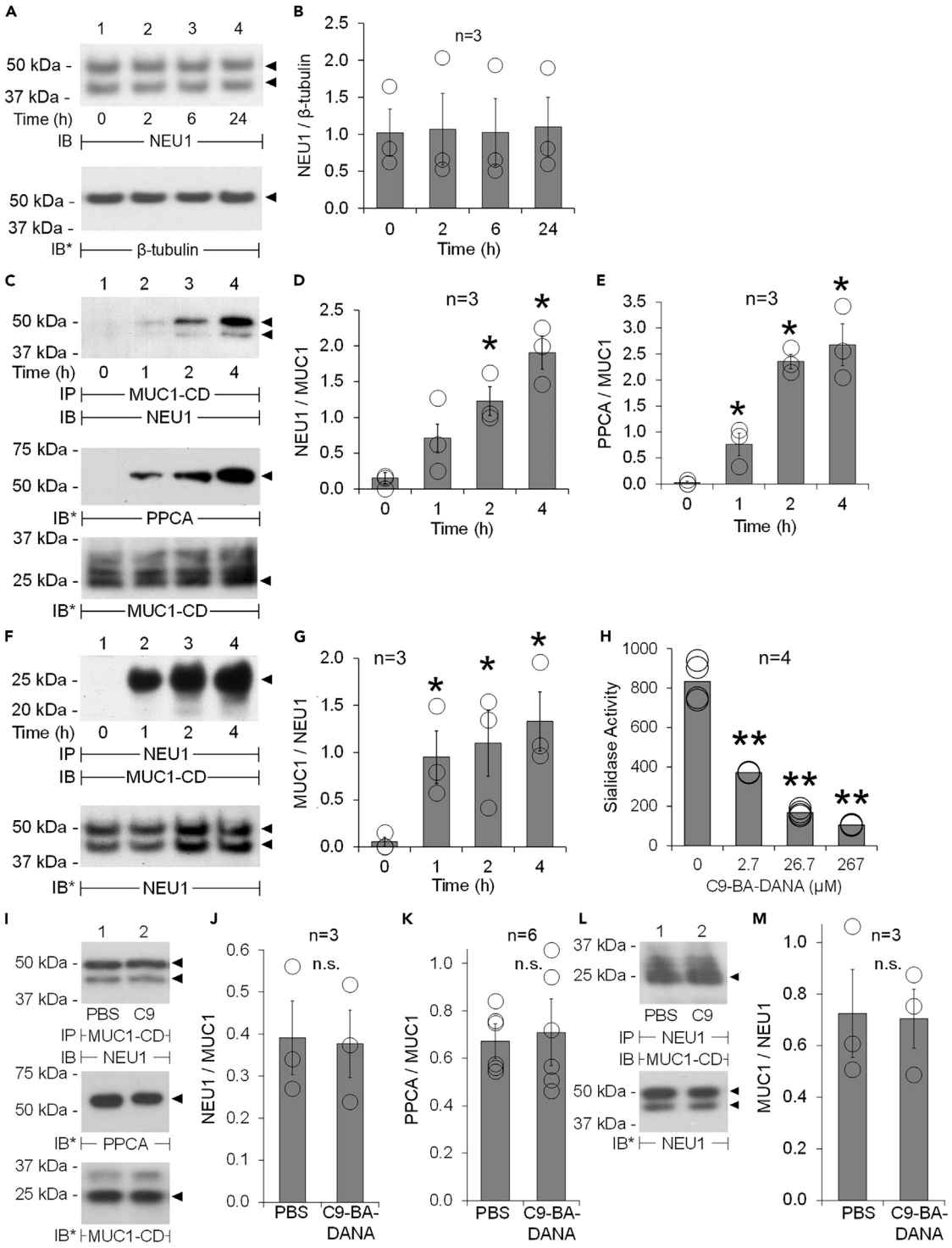

Figure 5. Sm increases NEU1 and PPCA association with MUC1

(A, C, and F) A549 cells were incubated with the PBS control for 4 h (lane 1) or Sm for 1 h (lane 2), 2 h (lane 3), or 4 h (lane 4). (A) Equal protein aliquots of cell lysates were immunoblotted with anti-NEU1 Ab. To control for protein loading and transfer, the blots were stripped and reprobed for anti-β-tubulin. (B) Densitometric analyses of NEU1 signals in (A) normalized to β-tubulin signals. (C and F) Equal protein aliquots of the lysates were immunoprecipitated (IP) with (C) anti-MUC1-CD Ab or (F) anti-NEU1 Ab. The MUC1-CD immunoprecipitates were processed for NEU1 or PPCA immunoblotting (C), while the NEU1 immunoprecipitates were processed for MUC1-CD immunoblotting (F). In each case, to control for protein loading and transfer, the blots were stripped and reprobed with the relevant immunoprecipitating Ab.

Figure 5. *Continued*

(D and E) Densitometric analyses of NEU1 (D) and PPCA (E) signals, each normalized to MUC1-CD signal. (G) Densitometric analyses of MUC1-CD signal normalized to NEU1 signal.

(H) A549 cells were incubated with increasing concentrations of the NEU1-selective sialidase inhibitor, C9-BA-DANA, and assayed for sialidase activity for the fluorogenic substrate, 4-MU-NANA, in arbitrary fluorescence units. Vertical bars represent mean ± SEM sialidase activity.

(I–K) The same reciprocal NEU1/PPCA-MUC1-CD co-immunoprecipitation assays were performed using cells pretreated with the PBS control (lane 1) or the NEU1-selective sialidase inhibitor, C9-BA-DANA (lane 2). Densitometric analyses of NEU1 (J) and PPCA (K) signals, each normalized to MUC1-CD signal, or the MUC1-CD signal (M) normalized to NEU1 signal. *, increased NEU1/PPCA association with MUC1 (D and E) or increased MUC1 association with NEU1 (G) compared to the medium control at $p < 0.05$. **, decreased sialidase activity (H) compared to the medium control at $p < 0.05$. n.s., not significant. Statistical comparisons were made using the Student's t test. The results are representative of 3, 4, or 6 independent experiments.

numbers of tandem repeats increasingly inhibited FliC1,2,3 binding to the MUC1-expressing cells (Figure 4I). Linear regression analysis revealed that the correlation between tandem repeat number and inhibition of flagellin binding was highly significant ($R^2 = 0.9955$, $p < 0.005$).

Sm Increases NEU1 and PPCA association with MUC1

We asked whether Sm engagement of MUC1 might increase association of NEU1 and/or its chaperone/transport protein, PPCA, with the MUC1 substrate. First, Sm exposure did not increase NEU1 protein expression in A549 cells over 2–24 h (Figures 5A and 5B). We then used reciprocal co-immunoprecipitation assays to screen for changes in NEU1-MUC1 and PPCA-MUC1 association. In Sm-exposed cells, immunoprecipitation of MUC1-CD time-dependently co-immunoprecipitated both NEU1 (Figures 5C and 5D) and PPCA (Figures 5C and 5E) and immunoprecipitation of NEU1 time-dependently co-immunoprecipitated MUC1-CD (Figures 5F and 5G). Sm increased association of NEU1 and PPCA with MUC1 as early as 1 h (Figures 5C, 5E–5G). However, at 1 h, the Sm-induced increase in MUC-CD co-immunoprecipitation of NEU1 did not achieve statistical significance ($p = 0.0559$) (Figure 5D). Compared to the 0 h controls, Sm stimulation at 4 h increased MUC1-NEU1 association 15.0-fold (Figure 5D) and 26.6-fold (Figure 5G), and increased MUC1-PPCA association 68.0-fold (Figure 5E).

We then asked whether NEU1 catalytic activity was required for Sm-induced MUC1-NEU1 and/or MUC1-PPCA association. We introduced the NEU1-selective sialidase inhibitor, C9-butyl-amide-2-deoxy-2,3-dehydro-N-acetylneuraminic acid (C9-BA-DANA),[43] to A549 cells and found that it dose-dependently inhibited total sialidase activity for the fluorogenic substrate, 2-(4-methylumbelliferyl)-α-D-N-acetylneuraminic acid (4-MU-NANA) (Figure 5H). Sm and A549 cells were co-cultured for 4 h in the presence of 267 μM (100 μg/mL) of C9-BA-DANA, after which the same co-immunoprecipitation assays were performed. Inhibition of NEU1 catalytic activity did not alter Sm-induced MUC1-NEU1 or MUC1-PPCA association compared to their respective PBS controls (Figures 5I–5M). Uncropped, replicate immunoblots corresponding to Figure 5A, 5C, 5F, 5I, and 5L are shown in Figures S5–S9. These combined data indicate that Sm adhesion to MUC1-expressing human airway epithelia rapidly increases MUC1 association with NEU1 and its chaperone, PPCA, and that NEU1 catalytic activity is not required for their increased association.

Sm Provokes NEU1-mediated MUC1-ED desialylation

Since exposure of A549 cells to Sm increases NEU1/PPCA-MUC1 association (Figures 5C–5G), we asked whether Sm might also provoke MUC1-ED desialylation. Peanut agglutinin (PNA) lectin was used to selectively probe for desialylated MUC1-ED. To validate the PNA lectin, we demonstrated that PNA recognized asialofetuin (Figure 6A, lane 2) but not sialylated fetuin (Figure 6A, lane 1). In supernatants of Sm-challenged cells, MUC1-ED desialylation was increased by 3.3-fold (Figure 6B, lane 2 vs. 1, 6C) and 9.2-fold (Figures 6D, lane 2 vs. 1 and 6E) compared to supernatants from PBS-treated ECs. In contrast, the cell-associated MUC1-ED in lysates from Sm-exposed cells was not more desialylated than was MUC1-ED from control cell lysates (Figures 6B, 6D, lane 4 vs. 3, 6C, 6E). Finally, we asked whether MUC1-ED desialylation was specifically mediated by NEU1. A549 cells were transfected with either NEU1-targeting or nontargeting control siRNAs (Figure 6F, lane 2 vs. 1), treated with Sm or PBS, and the supernatants incubated with PNA-agarose, and the PNA-bound proteins processed for MUC1-ED immunoblotting. In the supernatants from cells transfected with control siRNAs, Sm dramatically increased MUC1-ED desialylation compared to MUC1-ED in supernatants from the PBS control cells (Figures 6G, lane 2 vs. 1 and 6H). Prior silencing of NEU1 dramatically reduced Sm-induced MUC1-ED desialylation by 90.8% compared to the control siRNAs (Figures 6G, lane 4 vs. 2 and 6H). Uncropped, replicate lectin blots and immunoblots corresponding to Figures 6A, 6B, 6D, 6F, and 6G are shown in Figures S10–S14. These combined data indicate that (1) Sm increases MUC1-ED desialylation, (2) MUC1-ED desialylation is associated with its release from the cell surface, (3) cell-associated MUC1-ED is not desialylated, and (4) MUC1-ED desialylation is specifically and exclusively mediated by NEU1.

NEU1 regulates the Sm flagellin-MUC1-ED interaction

We asked whether altered NEU1 expression or catalytic activity might influence binding of the Alexa Fluor 594-labeled FliC1,2,3 flagellin mixture and/or Sm adhesion to MUC1-expressing human airway epithelia. A549 cells infected with an adenovirus (Ad) encoding for catalytically-active NEU1 (Ad-NEU1) exhibited dramatically increased NEU1 expression compared to ECs infected with an Ad expressing green fluorescent protein (GFP) as a vector control (Figure 7A, lane 2 vs. 1). Uncropped immunoblots corresponding to Figure 7A are shown in Figure S15. A549 cells were infected with Ad-NEU1 or the Ad-GFP vector control, incubated with increasing concentrations of the fluoroprobe-labeled FliC1,2,3 flagellin mixture, and flagellin binding determined. Compared to the vector control, NEU1 overexpression increased binding of the flagellin mixture to the ECs (Figure 7B). Scatchard transformation of the binding data indicated that NEU1 overexpression increased the binding affinity of the MUC1-ED-flagellin interaction by 4.2-fold without altering receptor number (Figure 7C). In

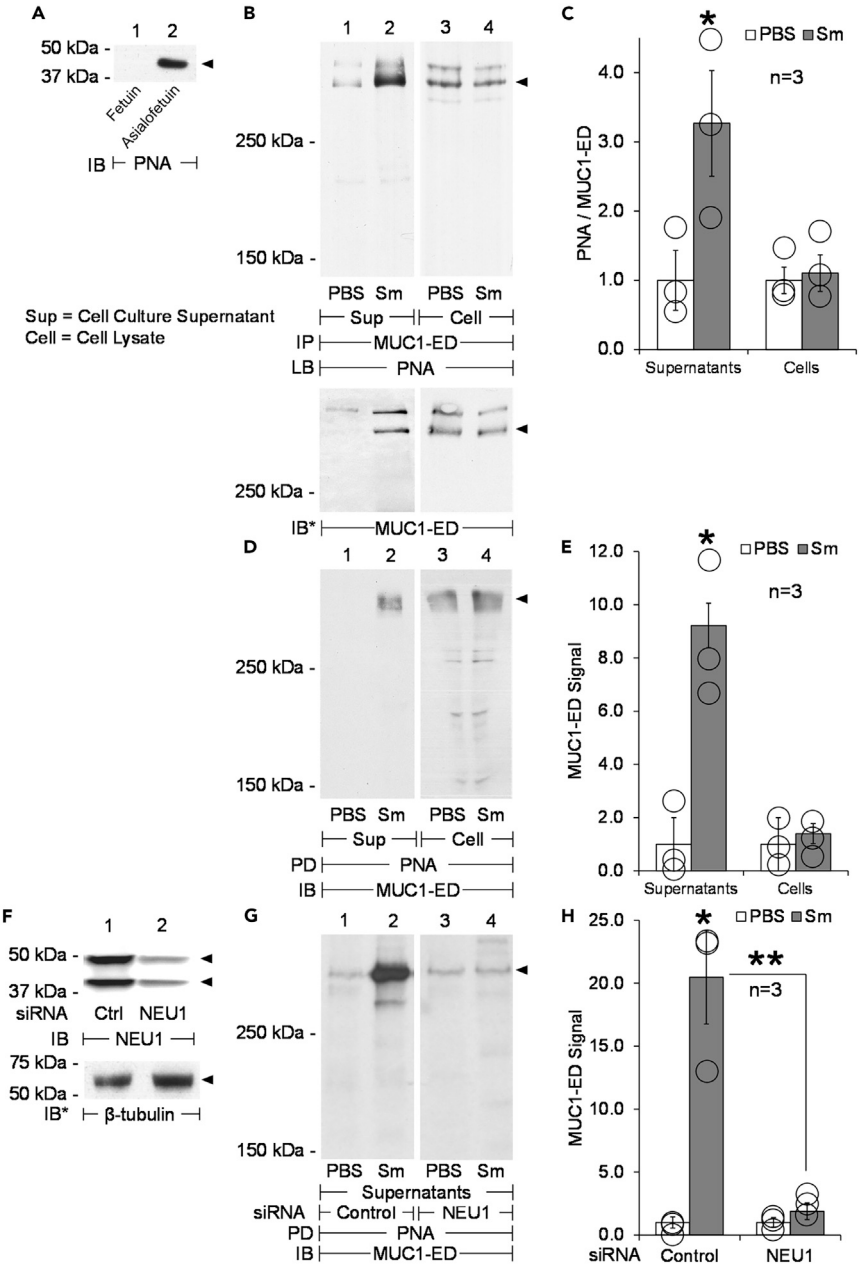

Figure 6. Sm provokes NEU1-mediated MUC1-ED desialylation

(A) Fetuin (lane 1) and asialofetuin (lane 2) were processed for PNA lectin blotting as negative and positive controls, respectively, to validate PNA specificity.

(B) A549 cells were incubated with the PBS control (lanes 1, 3) or Sm at MOI = 10^3 (lanes 2, 4). Equal protein aliquots of cell culture supernatants (lanes 1, 2) and cell lysates (lanes 3, 4) were immunoprecipitated with anti-MUC1-ED Ab and the MUC1-ED immunoprecipitates processed for PNA lectin blotting (LB). To control for protein loading and transfer, the blots were stripped and reprobed with the immunoprecipitating anti-MUC1-ED Ab.

(C) Densitometric analyses of PNA signal normalized to MUC1-ED signal.

(D) A549 cells were incubated with the PBS control (lanes 1, 3) or Sm at MOI = 10^3 (lanes 2, 4). Equal protein aliquots of cell culture supernatants (lanes 1, 2) and cell lysates (lanes 3, 4) were incubated with PNA-agarose and the PNA-binding proteins processed for MUC1-ED immunoblotting.

(E) Densitometric analyses of PNA-bound MUC1-ED signal.

(F) A549 cells were transfected with NEU1-targeting (lane 2) or nontargeting control (lane 1) siRNAs, lysed, and the lysates processed for NEU1 immunoblotting.

(G) A549 cells were transfected with nontargeting control (lanes 1, 2) or NEU1-targeting (lanes 3, 4) siRNAs and incubated with the PBS control (lanes 1, 3) or Sm at MOI = 10^3 (lanes 2, 4). Equal protein aliquots of cell culture supernatants were incubated with PNA-agarose and the PNA-binding proteins processed for MUC1-ED immunoblotting.

Figure 6. *Continued*

(H) Densitometric analyses of PNA-bound MUC1-ED signal. *, increased MUC1-ED desialylation (C, E, and H) compared to the PBS control at $p < 0.05$. **, decreased MUC1-ED desialylation compared to control siRNA (H) at $p < 0.05$. Statistical comparisons were made using the Student's t test. The results are representative of 3 independent experiments.

contrast, overexpression of either a catalytically-dead NEU1 mutant, NEU1-G68V,[44] containing a Gly[45]-to-Val substitution (Figure 7A, lane 3 vs. 1), or NEU3 (Figure 7A, lane 5 vs. 4), did not influence flagellin binding (Figure 7B and 7C). Silencing of endogenous NEU1 expression in human airway epithelia (Figure 6F, lane 2 vs. 1) diminished binding of the fluoroprobe-labeled FliC1,2,3 flagellin mixture (Figure 7D). Here, the binding affinity was diminished by 59.6%, whereas the receptor number was unchanged (Figure 7E). We then asked whether inhibiting the catalytic activity of NEU1, the predominant sialidase in human airway epithelia,[30] without altering its expression, might influence Sm flagellin binding to human airway epithelia. A549 cells were incubated with increasing concentrations of the fluoroprobe-labeled FliC1,2,3 flagellin mixture in the presence of C9-BA-DANA or the PBS control, and flagellin binding determined. Compared to the PBS control, inhibition of NEU1 catalytic activity decreased binding of the flagellin mixture to the ECs (Figure 7F). Scatchard analysis of the binding data indicated that NEU1 inhibition decreased the binding affinity by 79.9% without altering receptor number (Figure 7G).

Next, we asked whether these NEU1-mediated changes in flagellin binding might translate to changes in Sm adhesion to airway ECs. NEU1 overexpression (Figure 7A, lane 2 vs. 1) increased Sm adhesion to A549 cells 3.3-fold compared to Sm adhesion to cells infected with the vector control (Figure 7H). In contrast, overexpression of either NEU1-G68V, (Figure 7A, lane 3 vs. 1) or NEU3 (Figure 7A, lane 5 vs. 4) did not (Figure 7H). NEU1 knockdown decreased Sm adhesion by 57.4% compared to cells transfected with the nontargeting control siRNA (Figure 7I). We then introduced escalating concentrations of C9-BA-DANA to the Sm adhesion assay. C9-BA-DANA at concentrations $\geq$2.7 μM dose-dependently decreased Sm adhesion to airway epithelia (Figure 7J). Taken together, these combined data indicate that NEU1 catalytic activity dramatically increases Sm adhesion to human airway epithelia through increases in the binding affinity between Sm-expressed flagellin and the MUC1-ED receptor expressed on the surface of these same cells.

Sm provokes MUC1-ED shedding

After exposure of A549 cells to either Sm or the FliC1,2,3 flagellin mixture, cell culture supernatants were collected and MUC1-ED levels quantified by enzyme-linked immunosorbent assay (ELISA) and normalized to total EC protein. At MOIs of 0.1–10^3, Sm dose-dependently increased MUC1-ED shedding (Figure 8A). The Sm-provoked shedding could be detected as early as 2 h, with further time-dependent increments through 24 h compared to either pre-exposure shedding or the simultaneous PBS controls (Figure 8B). Exposure of A549 cells to PBS alone also was associated with small, but detectable, increases in MUC1-ED shedding at 12, 24, and 48 h compared to the 0 h control (Figure 8B). We then incubated Sm at MOI = 10^3 for 24 h with 1HAEo$^-$, CFTE29o$^-$, 16HBE14o$^-$, BEAS-2B, SAEC, or A549 cells and assayed for MUC1-ED shedding. Sm provoked comparable levels of MUC1-ED shedding from these epithelia derived from the entire length of the airway (Figure 8C). This pattern of Sm-induced MUC1-ED shedding paralleled airway epithelial NEU1 expression[30] and total cellular MUC1 expression (Figure 8C). As anticipated, MUC1-ED shedding was highly correlated with total cellular MUC1 expression ($R^2 = 0.9625$, $p < 0.001$) (Figure 8D). We then compared flagellin-expressing WT Sm and flagellin-null Sm for their abilities to provoke MUC1-ED shedding in A549 cells (Figure 8E) and SAECs (Figure 8F). The flagellin-null mutant induced 75.6% and 63.0% less MUC1-ED shedding in A549 cells and SAECs, respectively, compared to that observed for WT Sm. The WT Sm-induced MUC1-ED shedding from A549 cells was greater than that seen from SAECs (Figures 8C, 8E, and 8F). The purified Sm FliC1,2,3 flagellin mixture dose-dependently increased MUC1-ED shedding up to 8.6-fold compared to the simultaneous baseline control (Figure 8G). Isomolar concentrations of the 3 distinct Sm flagellin proteins, FliC1, FliC2, and FliC3, each promoted comparable levels of MUC1-ED shedding (Figure 8H). Sm-induced MUC1-ED desialylation was restricted to the soluble MUC1-ED pool released into the supernatant (Figures 6B–6E). We asked whether Sm-induced, NEU1-mediated MUC1-ED desialylation might promote MUC1-ED shedding. Prior silencing of NEU1 decreased Sm flagellin-provoked shedding by 79.8% compared to the simultaneous nontargeting siRNA control (Figure 8I). Similarly, inhibition of NEU1 catalytic activity with C9-BA-DANA decreased the Sm flagellin-induced shedding by 83.4% compared to the PBS control (Figure 8J).

Sialylation protects glycoproteins against proteolytic cleavage.[46,47] Three MUC1-ED sheddases have been identified in extrapulmonary tissues, including matrix metalloproteinase 14 (MMP14), a disintegrin and metalloprotease 17 (ADAM17), and ϒ-secretase.[48–50] Transcripts for MMP14 and ϒ-secretase, but not ADAM17, have been reported in airway epithelia.[51] In addition to these 2 classical MUC1-ED sheddases, elastase also reportedly cleaves MUC1.[8,52] We asked whether one or more of these 3 proteases expressed in airway epithelia, might be operative during Sm flagellin-induced MUC1-ED shedding. We screened 6 protease inhibitors, 2 of which are known to target each of these 3 proteases, at concentrations 10-fold and 100-fold greater than their reported IC_{50} values.[53–58] In each and every case, the protease inhibitors failed to block or diminish Sm-flagellin-induced shedding (Figure 8K and 8L). These results suggest that Sm-provoked MUC1-ED shedding cannot be ascribed to one or more of these 3 proteases.

The MUC1-ED contains an SEA domain within the membrane-proximal portion of its ectodomain.[1,2] Autoproteolysis occurs at the peptide bond between the Gly and Ser residues within a conserved G-S-V-V-V motif.[3–6] We asked whether the permissive effect of MUC1-ED desialylation on MUC1-ED shedding might involve the SEA domain. HEK293T cells expressing either a full-length rMUC1-WT, or a rMUC1-S317A mutant, containing a Ser[317]-to-Ala substitution at the Gly-Ser peptide bond, known to render the MUC1 protein resistant to autoproteolysis,[59] were studied. These same cells were exposed to Sm and assessed for MUC1-ED shedding. Shedding from the cells expressing the S317A mutation was reduced by 88.6% compared to rMUC1-WT-expressing cells (Figure 8M). These combined data indicate that (1) Sm dose- and time-dependently increases MUC1-ED shedding, (2) Sm-expressed flagellin is absolutely required and sufficient for

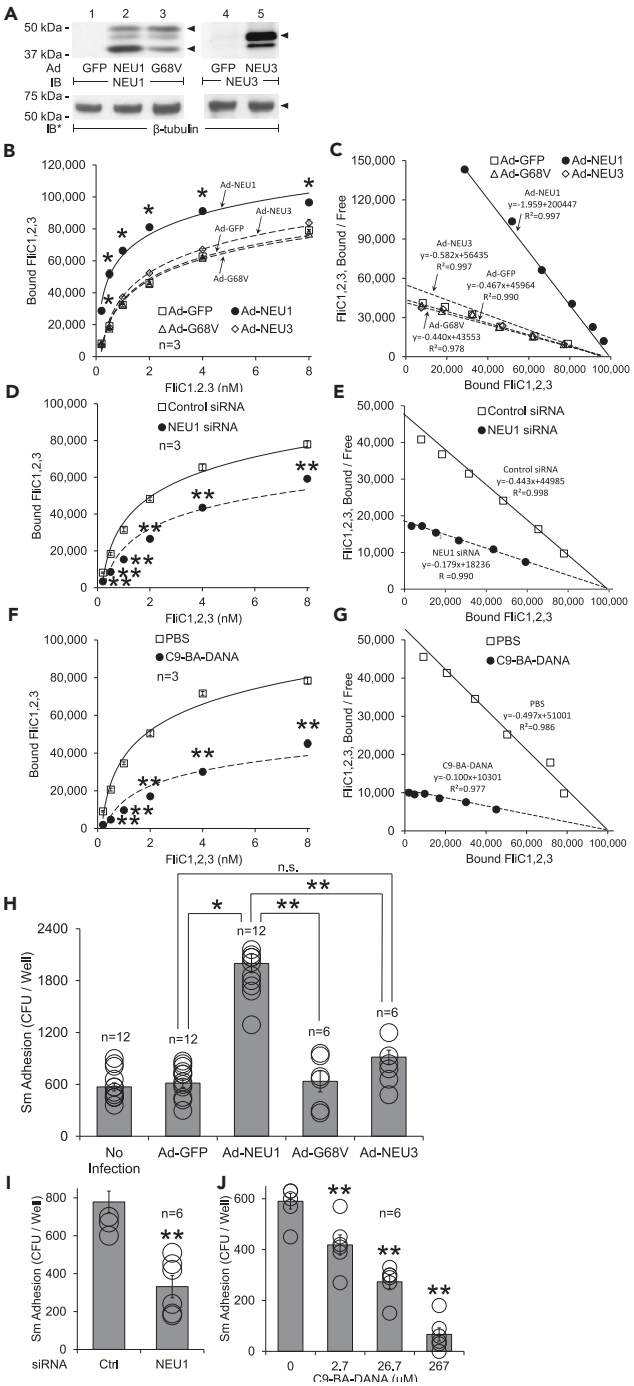

Figure 7. NEU1 sialidase regulates Sm flagellin binding and Sm adhesion to MUC1-expressing human airway epithelia

A549 cells were infected with Ad-NEU1, Ad-NEU1-G68V, Ad-NEU3, or Ad-GFP as the vector control, and incubated for 48 h.

(A) Ad-GFP- (lanes 1, 4), Ad-NEU1- (lane 2), Ad-NEU1-G68V- (lane 3), and Ad-NEU3- (lane 5) infected cells were lysed and the lysates processed for NEU1 (lanes 1–3) or NEU3 (lanes 4, 5) immunoblotting.

(B) The infected cells were incubated with increasing concentrations of the Alexa Fluor 594-labeled Sm flagellin mixture and bound flagellin determined.

(C) Scatchard analysis of binding data in (B).

(D and E) A549 cells were transfected with NEU1-targeting or control siRNAs and cultured for 48 h. (D) The transfected cells were incubated with increasing concentrations of the Alexa Fluor 594-labeled Sm flagellin mixture and bound flagellin determined. (E) Scatchard analysis of binding data in (D).

Figure 7. *Continued*

(F and G) A549 cells were treated with 267 μM of the NEU1-selective sialidase inhibitor, C9-BA-DANA, or PBS control. (F) The cells were incubated with increasing concentrations of the Alexa Fluor 594-labeled Sm flagellin mixture and bound flagellin determined. (G) Scatchard analysis of binding data in (F). (B, D, and F) Data points represent mean ± SEM bound flagellin in molecules/EC.

(H) The infected and noninfected cells, as described in (A, B, and C), were incubated with Sm and the cell-adherent Sm determined.

(I) The transfected cells, as described in (D and E), were incubated with Sm and the cell-adherent Sm determined.

(J) A549 cells were pre-incubated with increasing concentrations of C9-BA-DANA or PBS control. The cells were incubated with Sm and the cell-adherent Sm determined. (H, I, J) Vertical bars represent mean ± SEM Sm adhesion in CFUs/well. *, increased flagellin binding (B) or Sm adhesion (H) compared to the Ad-GFP vector control at $p < 0.05$. **, decreased flagellin binding or Sm adhesion compared to control siRNA (D and I), the PBS control (F and J), or Ad-NEU1 (H) at $p < 0.05$. n.s., not significant. Statistical comparisons were made using the Student's t test or ANOVA. The results are representative of 3, 6, or 12 independent experiments.

stimulating MUC1-ED shedding, (3) each of the 3 Sm flagellins increases shedding, (4) Sm-provoked shedding requires NEU1 catalytic activity, and (5) MUC1-ED shedding requires cleavage of the Gly-Ser peptide bond within its SEA domain.

Flagellin-expressing Sm increases MUC1-ED shedding into the bronchoalveolar compartment of mice and humans

We asked whether Sm and/or its flagellins might also increase MUC1-ED shedding *in vivo*. Mice were administered intranasally (i.n.) flagellin-expressing WT or flagellin-null Sm at 1.0×10^8 CFU/mouse or an equivalent volume of PBS vehicle alone. At 24 h post-challenge, BALF was collected and MUC1-ED levels quantified by ELISA and normalized to total BALF protein. In the BALF of WT Sm-challenged mice, the mean normalized MUC1-ED level was increased 32.6-fold, while the MUC1-ED level in the BALF of mice administered flagellin-null Sm was only increased 5.4-fold, each compared to their respective PBS controls (Figure 9A). The WT Sm-induced increase in MUC1-ED BALF levels was 6.1-fold greater than that seen after challenge with the flagellin-null Sm strain. Aliquots of BALF from these same Sm-challenged mice were centrifuged to pellet the bacteria, and the bacterial pellets processed for murine MUC1-ED immunoblotting. WT Sm pulled-down the MUC1-ED (Figures 9B, lanes 1–4, 9C), whereas flagellin-null Sm did not (Figures 9B, lanes 5–8 and 9C). These data indicate that the shed MUC1-ED retains its adhesiveness for flagellated Sm *in vivo* and that Sm flagellin expression is required for its binding to the shed MUC1-ED. Administration i.n. of the purified Sm FliC1,2,3 flagellin mixture increased the MUC1-ED level in BALF up 34.4-fold compared to the simultaneous PBS control (Figure 9D). BALF MUC1-ED desialylation in mice challenged i.n. with the FliC1,2,3 flagellin mixture increased 3.4-fold (Figures 9E, lanes 6–10 and 9F) compared to that seen in the PBS control-administered mice (Figures 9E, lanes 1–5 and 9F). Prior NEU1 inhibition with C9-BA-DANA reduced the Sm flagellin-induced MUC1-ED shedding by 95.1% compared to that seen in Sm flagellin-challenged mice given the PBS control (Figure 9G). Taken together, flagellated Sm and purified Sm-derived flagellins each provokes MUC1-ED shedding in mice, *in vivo*. Further, the shed, desialylated MUC1-ED retains its ability to bind flagellated Sm, and Sm flagellin-provoked MUC1-ED shedding is NEU1-dependent.

We then asked whether Sm-provoked, *in vivo* MUC1-ED shedding might be extended to Sm-infected humans. MUC1-ED levels were determined in BALFs collected from ventilated patients in which their BALFs either cultured positive for only Sm, for bacteria other than Sm, or were culture-negative, and each MUC1-ED level was normalized to total BALF protein in the same sample (Figure 10A). The mean normalized MUC1-ED concentration in the BALFs of Sm-infected patients was 17.6-fold higher than that found in the BALFs that cultured positive for bacteria other than Sm, and 25.2-fold higher than that found in BALFs from culture-negative patients. In reciprocal lectin blotting experiments, the level of desialylated MUC1-ED in BALF from Sm-infected patients was 4.1-fold (Figures 10B, lanes 5–8 and 10C) and 27.6-fold (Figures 10D, lanes 5–8 and 10E) higher than that seen in the culture-negative controls (Figures 10B and 10D, lanes 1–4). BALFs that cultured positive either for Sm or other bacteria were centrifuged to pellet the bacteria and the bacterial pellets processed for MUC1-ED immunoblotting. In BALF that cultured positive for Sm, the amount of MUC1-ED that was co-centrifuged with Sm was 5.7-fold greater (Figures 10F, lanes 5–8 and 10G) than that pulled down in BALF that cultured positive for bacteria other than Sm (Figures 10F, lane 1–4 and 10G). These findings indicate that ventilator-associated Sm pneumonia increases MUC1-ED desialylation and shedding, and that the shed MUC1-ED retains its adhesiveness for flagellin-expressing Sm.

Human rMUC1-ED functions as a flagellin-targeting decoy receptor, *in vitro*, and protects against lethal Sm lung infection, *in vivo*

We asked whether flagellin-provoked release of desialylated MUC1-ED from mucosal surfaces might benefit the host. We tested human rMUC1-ED-WT for its ability to inhibit flagellin-driven motility. The rMUC1-ED-WT molecule dose-dependently restrained Sm motility by up to 79.0% compared to the simultaneous PBS control (Figure 11A). In a biofilm assay where flagellin-expressing Sm were incubated with increasing concentrations of rMUC1-ED-WT, the rMUC1-ED-WT dose-dependently reduced biofilm formation by up to 77.7% (Figure 11B). When Sm were co-cultured with A549 cells in the presence of increasing concentrations of rMUC1-ED-WT, Sm adhesion to the airway epithelia was dose-dependently diminished by up to 86.9% (Figure 11C). However, when Sm were co-cultured with sections of PVC endotracheal tubes or polystyrene (PS) microwells, the rMUC1-ED-WT protein failed to reduce Sm adhesion to either substrate (Figure 11D). When the airway ECs were incubated with Sm in the presence of the same escalating concentrations of rMUC1-ED-WT, IL-8 levels in the culture supernatants were dose-dependently reduced by up to 63.6% (Figure 11E). In contrast, rMUC1-ED-WT displayed no effect on the growth of flagellin-expressing Sm compared to the PBS control (Figure 11F). The rMUC1-ED-WT molecule dramatically reduced binding of the fluoroprobe-labeled Sm FliC1,2,3 flagellin mixture to airway epithelia (Figures 11G and 11H). Compared to the PBS control, bound

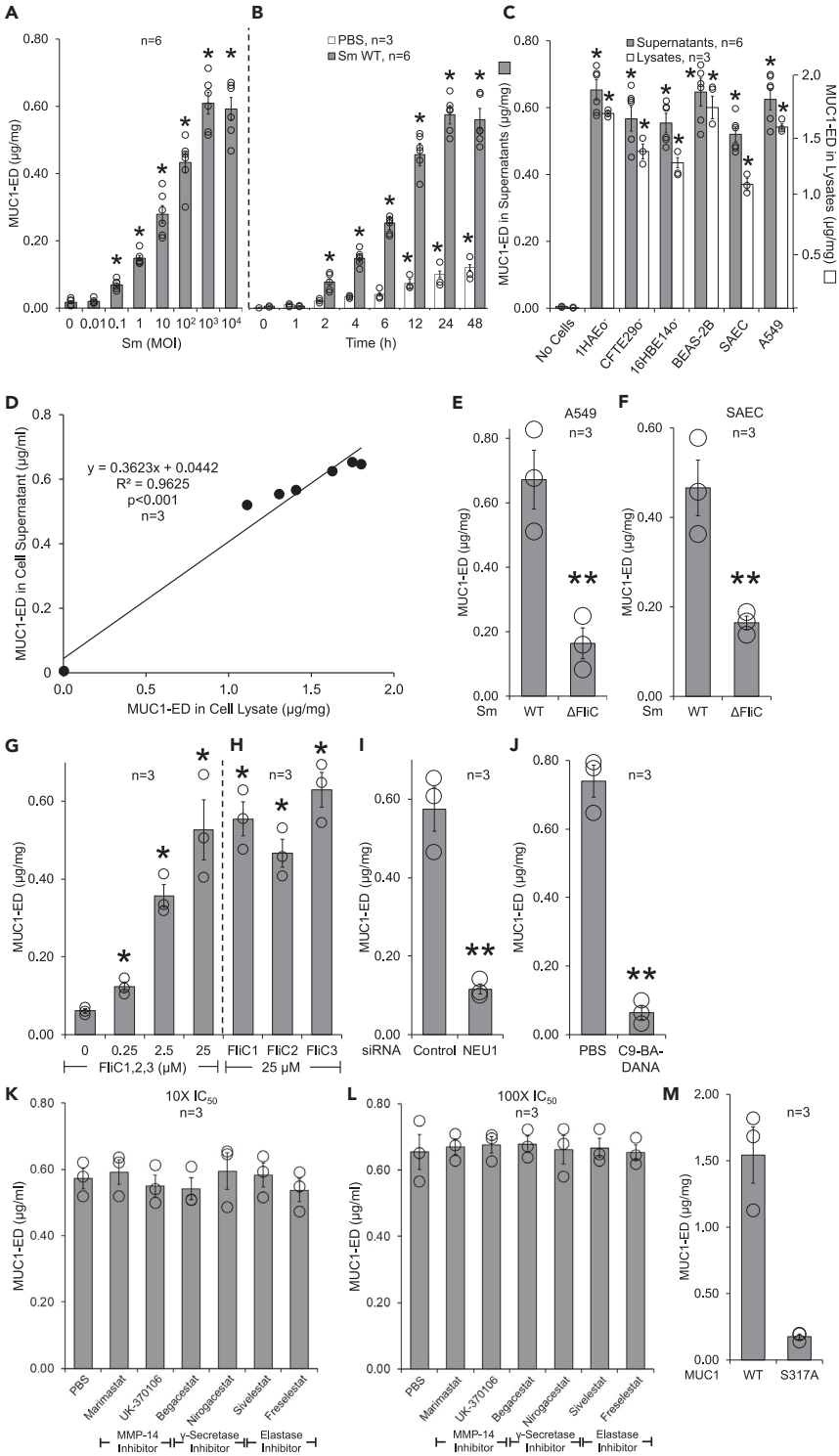

Figure 8. NEU1 regulates Sm flagellin-provoked MUC1-ED shedding

(A and B) A549 cells were incubated for (A) 24 h with increasing MOIs of Sm or the PBS control or (B) increasing times with the PBS control or Sm at an MOI of 10^3. (C) 1HAEo$^-$, CFTE29o$^-$, 16HBE14o$^-$, BEAS-2B, SAEC, and A549 cells, or a no cell control, were incubated with Sm for 24 h at an MOI of 10^3. MUC1-ED levels in cell culture supernatants (A–C) or cell lysates (C) were measured and normalized to total EC protein.

(D–J) Linear regression analysis of the correlation between MUC1-ED levels in 1HAEo$^-$, CFTE29o$^-$, 16HBE14o$^-$, BEAS-2B, SAEC, and A549 cell culture supernatants, each normalized to total EC protein, following incubation of the cells with Sm for 24 h at an MOI of 10^3, or the no cell control, and normalized

Figure 8. *Continued*

MUC1-ED levels in the corresponding cell lysates, or the no cell control. A549 cells (E) and SAECs (F) were incubated with flagellin-expressing WT Sm or flagellin-null Sm and normalized MUC1-ED levels in culture supernatants determined in μg/mg EC protein. A549 cells were treated with (G) increasing concentrations of the purified Sm FliC1,2,3, flagellin mixture or PBS control or (H) 25 μM of each of the individually purified FliC1, FliC2, or FliC3 flagellins, and normalized MUC1-ED levels in culture supernatants determined. A549 cells were transfected with NEU1-targeting or control siRNAs (I), or treated with the NEU1-selective inhibitor, C9-BA-DANA or PBS alone (J). The cells were stimulated with the Sm FliC1,2,3, flagellin mixture or PBS control and normalized MUC1-ED levels in culture supernatants determined.

(K and L) A549 cells were incubated for 24 h with Sm (MOI = 10^3) in the presence of the PBS control or inhibitors for MMP-14 (marimastat, UK-370106), γ-sceretase (begacestat, hirogacestat), or elastase (sivelestat, freselestat) at concentrations of 10X (K) or 100X (L) the reported IC_{50} of each inhibitor and normalized MUC1-ED levels in culture supernatants determined.

(M) HEK293T cells expressing either the WT rMUC1 or the rMUC1-S317A SEA domain cleavage-resistant mutant were stimulated with the Sm FliC1,2,3, flagellin mixture and normalized MUC1-ED levels in culture supernatants determined. Vertical bars represent mean ± SEM normalized MUC1-ED levels in μg/mg protein. *, increased mean normalized MUC1-ED levels compared to (A, G, H) the PBS controls, (B) the simultaneous PBS controls at each Sm exposure time, or (C) the simultaneous no cell controls at $p < 0.05$. **, decreased mean normalized MUC1-ED levels compared to WT Sm (E and F), control siRNA (I), PBS control (J), or WT MUC1 expression (M) at $p < 0.05$. Statistical comparisons were made using the Student's t test. The results are representative of 3 or 6 independent experiments.

flagellin, i.e., receptor occupancy, was decreased by 95.3% without altering binding affinity (Figure 11H). Therefore, the rMUC1-ED-WT protein dramatically disrupts a diverse array of *in vitro* Sm flagellin-driven processes essential for Sm pathogenicity.

We then tested the ability of rMUC1-ED-WT to protect against lethal Sm lung infection, *in vivo*. First, we determined the Sm inoculum size required to establish a lethal lung infection. Mice were administered i.n. with $1.0x10^9$, $1.0x10^{10}$, or 1.0×10^{11} CFU/mouse of Sm and survival followed for 7 days. At 7 days post-infection (Figure 11I), mice administered i.n. with 1.0×10^9 CFU per mouse of Sm exhibited 100% survival, mice administered i.n. with 1.0×10^{10} CFU had 50% survival, and administration of 1.0×10^{11} CFU resulted in 0% survival. Next, the rMUC1-ED-WT (100 μg/g body weight) or PBS control were co-administered i.n. to mice together with 1.0×10^{11} CFU/mouse of Sm and survival was followed for 7 days. At 7 days post infection (Figure 11J), mice co-administered with flagellin-expressing Sm and the rMUC1-ED-WT protein exhibited 71.4% survival versus 14.3% survival in mice co-administered with Sm plus the PBS control. These data demonstrate that the human rMUC1-ED-WT protein protects against lethal murine Sm lung infection and support the potential therapeutic value for *E. coli*-expressed rMUC1-ED-WT for human invasive Sm lung infections.

DISCUSSION

Bacterial adhesion to the host epithelial surface is mediated through one or more bacterial adhesins and their cognate host cell receptors.[14,16,60] We first asked whether Sm might reach out to and cross-talk with host airway epithelia through its flagella. In one report, flagellin-expressing WT Sm displayed greater adhesion to HEK293T cells than did flagellin-null bacteria.[20] In the current studies we found that the flagellin-null Sm mutant also displays profoundly reduced adhesion to either of 2 distinct human airway epithelia compared to WT Sm. Further, WT Sm adhesion was dose-dependently reduced in the presence of increasing concentrations of either a purified Sm FliC1,2,3 flagellin mixture or each individual flagellin protein. Our structural analyses of select bacterial flagellins, including the 3 Sm flagellins, suggest that 3 conserved aa's (Val-206, Asp-207, and Lys-220), and/or the groove in the D2 domain between the β-sheet and α-helix, of the Sm flagellins participate in bacterial adhesion to host ECs. These combined data establish the 3 Sm flagellins as adhesins required for Sm adhesion to the human airway epithelium.

Overexpression of the established pattern recognition receptor for bacterial flagellin, TLR5,[38] in HEK293T cells did not increase their adhesiveness for Sm. Further, multiple flagellated bacteria known to activate TLR5 each reportedly failed to provoke MUC1-ED shedding.[23] Another receptor that we considered for flagellated Sm was the MUC1-ED. In fact, multiple flagellated bacteria, including, Pa, *Heliobacter pylori*, *Campylobacter jejuni*, *E. coli*, *Salmonella enterica*, and *Yersinia pseudotuberculosis*,[8–12] each reportedly binds to the MUC1-ED. In the current studies, we found that MUC1 overexpression increased the binding of the FliC1,2,3 flagellin mixture and Sm bacteria to airway epithelial and HEK293T cells, whereas siRNA-induced silencing of MUC1 dramatically reduced these same 2 endpoints. As a quantifiable biochemical endpoint for intracellular signaling downstream to the MUC1-ED—flagellin receptor-ligand interaction,[42] the FliC1,2,3 flagellin mixture increased ERK1/2 activation compared to the PBS control, and prior silencing of MUC1 dramatically reduced the flagellin-provoked ERK1/2 activation compared to the nontargeting siRNA control. Therefore, the Sm-derived flagellins constitute signal-transducing ligands for the MUC1 host receptor, and activation of ERK1/2 by these flagellins is predominantly transduced through MUC1.

When *E. coli*-expressed recombinant proteins corresponding to MUC1-ED-WT, or the MUC1-ED-Δ1 and MUC1-ED-Δ2 deletion mutants, were screened for their ability to block binding of the FliC1,2,3 flagellin mixture to MUC1-expressing airway epithelia, only tandem repeat-containing proteins were inhibitory. The tandem repeat-containing proteins directly bound to the Sm flagellins. Previous studies have demonstrated that multiple MUC1-ED tandem repeats are required for the MUC1-ED to assume the tertiary structure necessary for its bioactivity.[61–63] Biophysical measurements have demonstrated that a single MUC1-ED tandem repeat adopts a random coil structure in solution, whereas ≥3 tandem repeats adopt a stable, rod-shaped conformation (60). Other investigators screened synthetic peptides corresponding to increasing numbers of MUC1-ED tandem repeats, to either suppress the human T-lymphocyte proliferative response,[62] or to block binding of human intracellular adhesion molecule-1 to MUC1.[63] They observed that peptides corresponding to ≥3 tandem repeats were inhibitory and that inhibitory activity was directly proportional to the number of repeats present in the peptide. The results of these studies are in agreement with our current findings. These combined data indicate that multimeric tandem repeats within the MUC1-ED adopt a rod-like bioactive

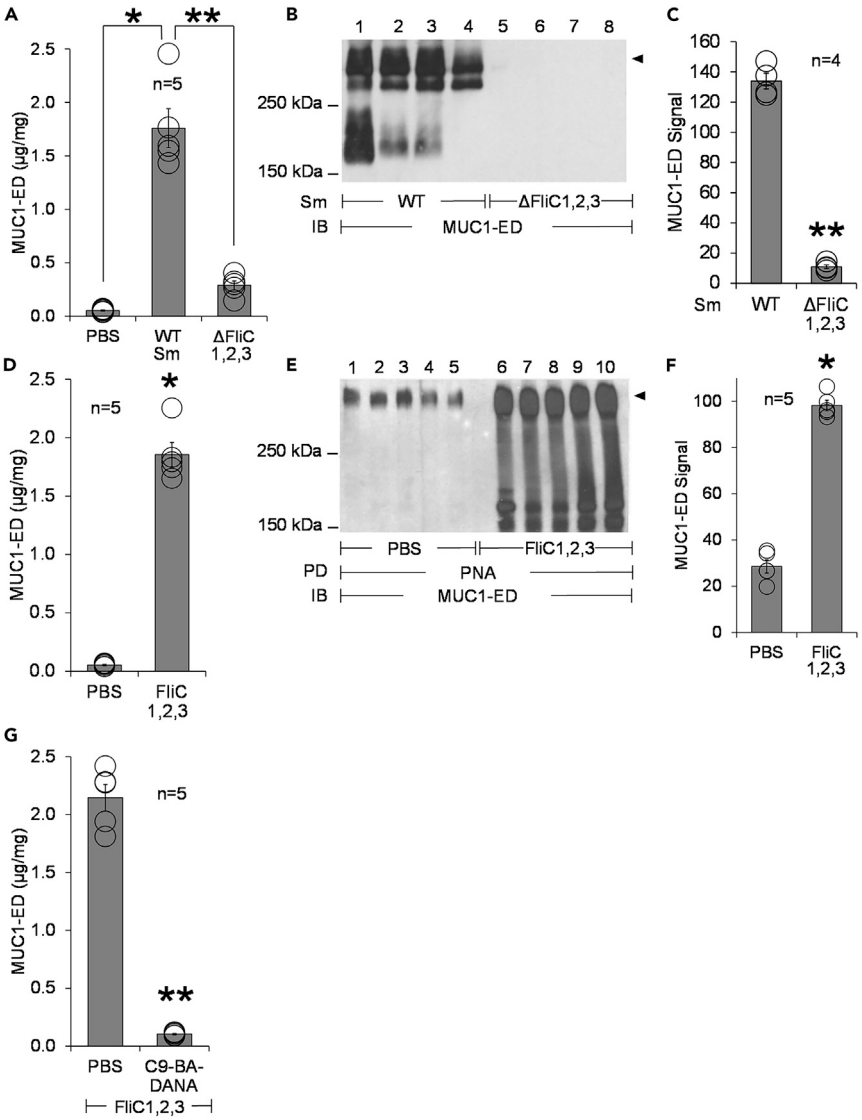

Figure 9. Flagellin-expressing Sm provokes MUC1-ED shedding in the airways of mice *in vivo*

(A) DBA/2 mice were administered i.n. the PBS control, flagellin-expressing WT Sm, or flagellin-null Sm, and MUC1-ED levels in BALF measured and normalized to total BALF protein.

(B) BALFs from DBA/2 mice administered i.n. with WT (lanes 1–4) or flagellin-null (lanes 5–8) Sm were centrifuged and the bacterial pellets processed for MUC1-ED immunoblotting.

(C) Densitometric analysis of the bacteria-associated MUC1-ED signal in the blots in (B).

(D) DBA/2 mice were administered i.n. the PBS control or the Sm FliC1,2,3 flagellin mixture and normalized MUC1-ED levels in BALF determined.

(E) BALFs from DBA/2 mice administered i.n. with the PBS control (lanes 1–5) or Sm FliC1,2,3 flagellin mixture (lanes 6–10) were incubated with PNA-agarose and the PNA-binding proteins processed for MUC1-ED immunoblotting.

(F) Densitometric analyses of the PNA-bound MUC1-ED signals in the blots in (E).

(G) DBA/2 mice were administered intraperitoneally (i.p.) with 170 nmol/g body weight of the PBS control or the NEU1-selective sialidase inhibitor, C9-BA-DANA. After 24 h, the mice were administered with the same dose of inhibitor or PBS control and administered i.n. with the Sm FliC1,2,3 flagellin mixture. After an additional 24 h, normalized MUC1-ED levels in BALF were determined. (A, D, and G) Vertical bars represents mean ± SEM normalized MUC1-ED levels in µg/mg protein. (C and F) Vertical bars represents mean ± SEM MUC1-ED signal. *, increased mean normalized MUC1-ED level (A and D) or MUC1-ED signal (F) compared to the PBS control at $p < 0.05$. **, decreased mean normalized MUC1-ED level (A and G) or MUC1-ED signal (C) compared to WT Sm or the PBS control at $p < 0.05$. Statistical comparisons were made using the Student's t test. The results are representative of 4 or 5 independent experiments.

conformation that can recognize and respond to multiple ligands, including the 3 Sm-expressed flagellins. Although monomeric flagellin clearly binds to the rMUC1-ED-WT molecule containing multimeric tandem repeats, the magnitude of this binding is likely greater than that measured here, given the potential polyvalent interactions between multimeric flagellins within the bacterial flagellar filament and

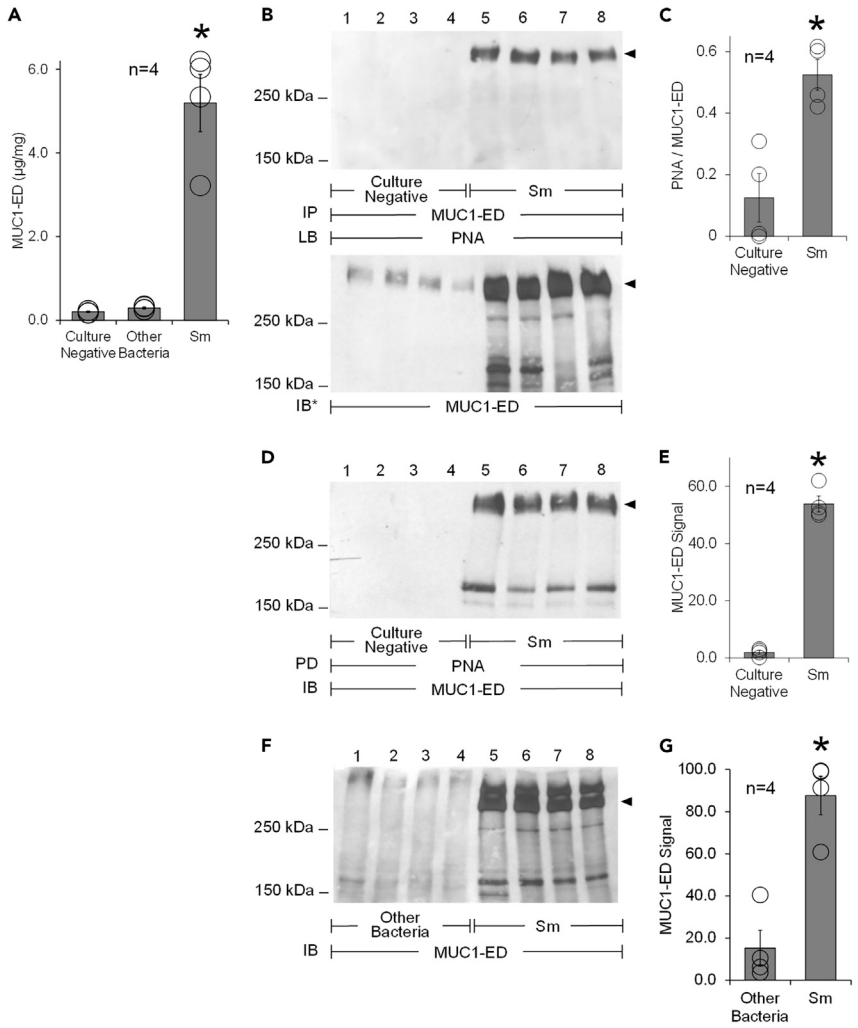

Figure 10. Sm provokes MUC1-ED desialylation and shedding in the airways of patients with ventilator-associated Sm pneumonia

(A) BALFs were obtained from hospitalized patients with ventilator-associated pneumonia that cultured positive for either Sm or bacteria other than Sm, or from culture-negative ventilated patients. MUC1-ED levels in BALFs were quantified by ELISA and normalized to total BALF protein. Vertical bars represent mean ± SEM normalized MUC1-ED levels in µg/mg protein.

(B) BALFs that were culture negative (lanes 1–4) or cultured positive for Sm (lanes 5–8) were immunoprecipitated with anti-MUC1-ED Ab and the MUC1-ED immunoprecipitates processed for PNA lectin blotting. To control for protein loading and transfer, the blots were stripped and reprobed for MUC1-ED.

(C) Densitometric analyses of PNA signal normalized to MUC1-ED signal in the blots in (B). Vertical bars represent mean ± SEM normalized PNA signal.

(D) The same BALFs from (B) were incubated with PNA-agarose and the PNA-bound proteins processed for MUC1-ED immunoblotting.

(E) Densitometric analyses of PNA-bound MUC1-ED signal of the blots in (D).

(F) BALFs that cultured positive for bacteria other than Sm (lanes 1–4) or cultured positive for Sm (lanes 5–8) were centrifuged and the bacterial pellets processed for MUC1-ED immunoblotting.

(G) Densitometric analysis of bacteria-associated MUC1-ED signal in the blots displayed in (F). (E and G) Vertical bars represent mean ± SEM MUC1-ED signal. *, increased mean normalized MUC1-ED level (A), normalized PNA signal (C), PNA-associated MUC1-ED signal (E), or bacteria-associated MUC1-ED signal (G) compared to culture-negative BALFs or BALFs culture positive for bacteria other than Sm at $p < 0.05$. Statistical comparisons were made using the Student's t test. The results are representative of 4 independent experiments.

the multiple tandem repeats within the MUC1-ED. Whether cell-associated and/or shed MUC1 molecules with more tandem repeats exhibit greater adhesiveness for flagellated Sm and Pa, or whether individuals expressing MUC1 with different tandem repeat numbers have altered susceptibility to bacterial colonization and/or invasive infection is unknown.

The MUC1-ED receptor is central to our hypothetical model for Sm and Pa binding to airway epithelial cells (Figure 12). However, Sm also binds to abiotic surfaces, and colonizes and infects indwelling plastic catheters, mechanical ventilators, nebulizers, hemodialysis circuits, and prostheses.[34] Accordingly, Sm adhesion to a number of artificial substrates has been studied. To varying degrees, Sm binds to PS plastic,[35,64,65] as well as glass and Teflon.[66] Other investigators compared Sm adhesion to PS with its adhesion to borosilicate glass and

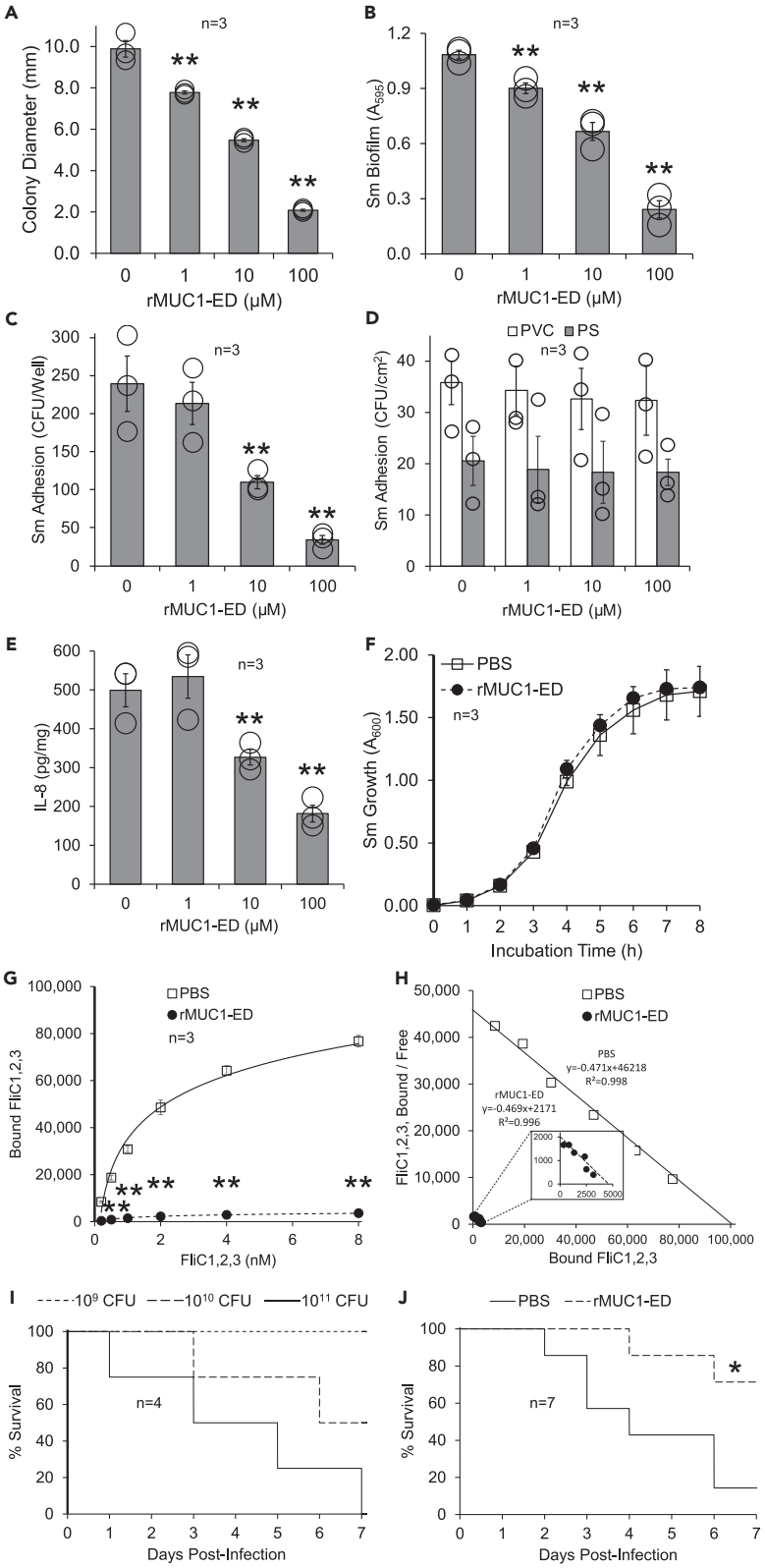
A
n=3
Colony Diameter (mm)
rMUC1-ED (μM)
B
n=3
Sm Biofilm (A595)
rMUC1-ED (μM)
C
n=3
Sm Adhesion (CFU/Well)
rMUC1-ED (μM)
D
PVC PS
n=3
Sm Adhesion (CFU/cm2)
rMUC1-ED (μM)
E
n=3
IL-8 (pg/mg)
rMUC1-ED (μM)
F
PBS
rMUC1-ED
n=3
Sm Growth (A600)
Incubation Time (h)
G
PBS
rMUC1-ED
n=3
Bound FliC1,2,3
FliC1,2,3 (nM)
H
PBS
rMUC1-ED
PBS
y=-0.471x+46218
R2=0.998
rMUC1-ED
y=-0.469x+2171
R2=0.996
FliC1,2,3, Bound / Free
Bound FliC1,2,3
I
10^9 CFU
10^10 CFU
10^11 CFU
n=4
% Survival
Days Post-Infection
J
PBS
rMUC1-ED
n=7
% Survival
Days Post-Infection

Figure 11. Human rMUC1-ED functions as a flagellin-targeting decoy receptor with antibacterial and anti-inflammatory properties *in vitro*, and protects against lethal Sm lung infection, *in vivo*

(A–D) Increasing concentrations or rMUC1-ED-WT, aa1-375, or the PBS control were incubated with Sm, and the bacteria assayed for (A) motility and (B) biofilm formation, or adhesion to (C) A549 cells or (D) sections of PVC endotracheal tubes, or PS cell culture wells.

(E) The culture supernatants were assayed for IL-8 levels and normalized to total EC protein. (A–E) Vertical bars represent mean ± SEM Sm motility in mm, Sm biofilm formation in A_{595} values, Sm adhesion in CFUs/well, or normalized IL-8 levels in pg/mg protein.

(F) Sm were cultured in LB medium in the presence of 100 μM of rMUC1-ED-WT or PBS control and assayed for bacterial growth. Data points represent mean ± SEM A_{600} values.

(G) A549 cells were incubated with increasing concentrations of the Alexa Fluor 594-labeled Sm flagellin mixture in the presence of 100 μM of rMUC1-ED-WT or PBS control, and bound flagellin determined. Data points represent mean ± SEM bound flagellin in molecules/EC.

(H) Scatchard analysis of binding data in (G). The insert magnifies the clustered values for the rMUC1-ED-treated flagellin.

(I) DBA/2 mice were administered i.n. with increasing CFUs of WT Sm and survival followed for 7 days.

(J) DBA/2 mice were co-administered i.n. 1.0×10^{11} CFU/mouse of WT Sm with 100 μg/g body weight of rMUC1-ED-WT or PBS control, and survival followed for 7 days *, increased survival (J) compared to the PBS control at $p < 0.05$. **, decreased Sm motility (A), biofilm formation (B), adhesion (C), IL-8 release (E), or flagellin binding (G) compared to the respective PBS controls at $p < 0.05$. Statistical comparisons were made using the Student's t test or the Mantel-Cox log rank test. The results are representative of 3, 4, or 7 independent experiments.

polypropylene plastic.[67] Sm adhesion to PS exceeded that seen to the other 2 materials. Whether flagellin is involved in Sm adhesion to one or more plastics is unclear. Although plastic cannot intrinsically express MUC1, it may become coated with shed MUC1-ED-containing mucus.[17] In one study, ultrastructural analysis by scanning electron microscopy of Sm adhering to plastic coverslips revealed flagella-like structures.[37] In another study, anti-flagellin Ab reduced Sm adhesion to PS in a dilution-dependent manner.[66] In the current studies, we examined a plastic material highly relevant to ventilator-associated Sm pneumonia, PVC-derived endotracheal tubes.[68] Sm adhesion to PVC surpassed that observed for PS. However, Sm adhesion to 6 distinct airway epithelia exceeded that seen for PVC. When adhesion of flagellin-expressing WT Sm was compared to flagellin-null Sm, the flagellated bacteria displayed greater adhesion to the airway epithelia, but this was not the case for Sm adhesion to PVC. These data indicate that although Sm flagellins are required for bacterial adhesion to host cells, they do not contribute to its adhesion to PVC. Further evidence that Sm flagellins do not contribute to Sm adhesion to PVC is the observation that the flagellin-targeting, rMUC1-ED decoy receptor that completely blocks flagellin binding and Sm adhesion to airway epithelia, does not inhibit Sm adhesion to PVC or PS.

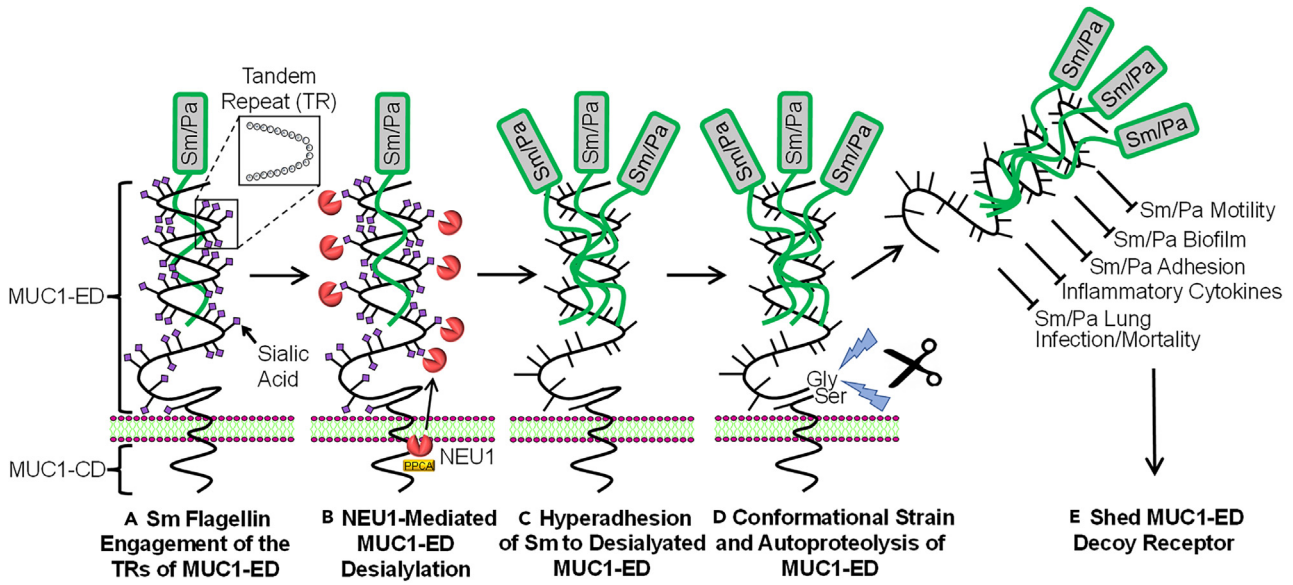

Figure 12. Hypothetical model for Sm/Pa flagellin-provoked shedding of the flagellin-targeting, MUC1-ED decoy receptor from the airway epithelial surface

(A) Sm/Pa flagellin engages the tandem repeats of the MUC1-ED.

(B) This receptor-ligand interaction increases NEU1/PPCA association with and desialylation of the MUC1-ED.

(C) NEU1-mediated MUC1-ED desialylation unmasks cryptic binding sites for Sm/Pa flagellin, enhancing flagellin binding and Sm/Pa adhesion to MUC1-expressing airway epithelia.

(D) This rapid, extensive MUC1-ED desialylation exerts conformational stress that catalyzes autoproteolysis at the Gly-Ser bond within the SEA domain, permitting MUC1-ED release from the airway epithelial surface into the airway lumen.

(E) The shed, soluble MUC1-ED retains its hyperadhesiveness for Sm/Pa flagellin to function as a flagellin-targeting decoy receptor that reduces Sm motility, biofilm formation, and adhesion to airway EC-associated MUC1-ED, and IL-8 production, *in vitro*, and protects against lethal Sm/Pa lung infection, *in vivo*.

Approximately 80% of the more than 500 predicted MUC1-ED O-linked glycosylation sites generate glycan chains that terminate in sialic acid.[45] Sialic acid is bulky and negatively charged, and in its terminal position can introduce steric hindrance and electrostatic repulsion.[69,70] These properties allow high levels of sialylation to mask cryptic binding sites or receptors from their binding partners or ligands. However, we found robust Sm adhesion to MUC1-expressing airway epithelia. We asked whether Sm might exploit NEU1, the predominant sialidase expressed in human airway epithelia and whose expression spatially correlates with that known for MUC1 expression,[30] to enhance the Sm flagellin-MUC1-ED interaction. We found that Sm rapidly increases MUC1 association with both NEU1 and PPCA, implicating Sm-provoked mobilization of a preformed NEU1 pool. In the supernatants of airway epithelia co-cultured with Sm, soluble MUC1-ED was consistently desialylated, whereas desialylation of cell-associated MUC1-ED could not be detected. That desialylation was evident for the soluble extracellular MUC1-ED, but not the cell-associated MUC1-ED, raised the question as to whether MUC1-ED desialylation may play a permissive or causal role in its release. Prior silencing of NEU1 almost completely protected against both Sm-induced MUC1-ED desialylation and shedding. These combined data indicate that NEU1 is required for MUC1-ED desialylation, which in turn, is required for its release from the cell surface.

We asked whether NEU1 might regulate the interaction between Sm and/or its flagellins with the MUC1-ED. NEU1 overexpression increased binding of the Sm FliC1,2,3 flagellin mixture to MUC1-expressing epithelia through increased binding affinity, without increasing receptor number, and dramatically increased Sm adhesion to these same cells. As anticipated, silencing of NEU1 and inhibition of NEU1 catalytic activity each dramatically reduced both binding of the Sm FliC1,2,3 flagellin mixture and Sm adhesion. Prokaryotic neuraminidases are established virulence factors for viral and bacterial pathogens.[71] To our knowledge, Sm does not express a neuraminidase. Rather, this prokaryotic organism recruits a eukaryotic sialidase, NEU1, to enhance its own adhesion to host tissues, and possibly, its overall pathogenicity. These same findings have been observed for another flagellated, NEU-deficient bacterium, Pa.[21–23]

In a mouse model, we have extended Sm-induced MUC1-ED shedding, *in vitro*, to an intact animal model. Flagellin was necessary and sufficient, and NEU1 catalytic activity was required. The shed MUC1-ED was desialylated and retained its adhesiveness for Sm flagellins. Finally, in patients with ventilator-associated Sm pneumonia, BALF levels of shed MUC1-ED were dramatically elevated compared to that found in patients with BALF culture-positive for bacteria other than Sm, or with culture-negative BALFs. Again, the shed MUC1-ED was desialylated and retained its adhesiveness for Sm flagellins. Taken together, our human *in vitro* and murine *in vivo* studies can be extended to *in vivo* human pathophysiology. Measurement of MUC1-ED levels may offer a rapid, reliable means to identify ventilated patients with Sm pneumonia that could serve as a guide for empiric antibiotic therapy to target this increasingly, intrinsically MDR pathogen.

The mechanism(s) through which Sm and its flagellins increase MUC1-ED shedding is unclear. Sialylation masks protease recognition sites and protects glycoproteins against proteolysis.[46,47] NEU1-mediated desialylation is required for Sm/flagellin-provoked MUC1-ED shedding. One would predict that MUC1-ED desialylation would increase its susceptibility to proteases. However, at concentrations up to 100-fold greater than their reported IC_{50} values, multiple inhibitors that target the 3 lung-expressed proteases reported to proteolytically release the MUC1-ED from the cell surface,[8,49,50,52] failed to block or diminish Sm/flagellin-provoked shedding. To address whether autoproteolysis at the Gly-Ser bond within the MUC1-ED SEA domain was required for Sm/flagellin-induced MUC1-ED shedding, a full-length rMUC1 and a rMUC1-S317A mutant[59] resistant to SEA autoproteolysis each was overexpressed in HEK293T cells and the manipulated cells treated with the Sm FliC1,2,3 flagellin mixture. In the cells overexpressing the S317A mutant, MUC1-ED shedding was almost nonexistent. This observation indicates that disruption of the Gly-Ser bond within the SEA domain is absolutely required for Sm/flagellin-induced MUC1-ED shedding. Several biophysical studies have demonstrated that MUC1 SEA domain autoproteolysis is catalyzed by conformational stress.[3–6,72] Changes in sialylation are known to alter intramolecular bonds, glycan chain flexibility, and glycoprotein conformation.[73–75] More specifically, removal of sialic acid induces conformational changes in human serum amyloid P, α_2 macroglobulin, β_1 integrin, α_1 acid glycoprotein, K^+ and Na^+ channels, and erythropoietin.[76–81] Even more relevant to this discussion, NEU1-mediated desialylation itself reportedly promotes conformational changes in the insulin receptor in both HEK293T cells and C57BL/6 mice, and β2-integrin in human neutrophils.[82,83] Each MUC1 molecule contains hundreds of bulky, negatively-charged sialic acid molecules.[1,2,13] We propose that rapid and extensive NEU1-mediated, MUC1-ED desialylation introduces conformational stress, which in turn, catalyzes SEA autoproteolysis, with cleavage at the Gly-Ser bond, a prerequisite event for flagellin-provoked MUC1-ED shedding.

Sm-expressed flagellins constitute virulence factors that increase Sm motility, Sm adhesion to host epithelia and mucus, biofilm formation, and proinflammatory gene expression.[17,20,84] One would predict that a host response that disrupts one or more of these flagellin-driven processes would protect against flagellin-mediated Sm pathogenicity. Human rMUC1-ED directly binds to the Sm-expressed flagellins and shed MUC1-ED retains its hyperadhesiveness for Sm. At MUC1-ED concentrations comparable to those found in the BALFs of Sm-infected patients, the flagellin-targeting, *E. coli*-expressed human rMUC1-ED dose-dependently reduced Sm motility, biofilm formation, adhesion to airway epithelia, as well as IL-8 production. Blockade of these flagellin-driven events might conceivably help the host to contain a bacterial infection. In fact, co-administration of human rMUC1-ED with a lethal dose of Sm increased 7-day survival of mice from 14.3% to 71.4%. However, the human rMUC1-ED exerted no detectible bacteriostatic or bactericidal activities for Sm. The mechanism of action of many conventional antibiotics requires bacterial replication and cell wall remodeling.[36] It is possible that human rMUC1-ED, which itself does not alter bacterial replication, might be combined with antibiotics for synergistic therapy against MDR flagellated pathogens.

The current data establish a novel host defense mechanism in response to select flagellated, NEU-deficient bacteria, such as Sm and Pa, with generation of a flagellin-targeting, MUC1-ED decoy receptor at the airway epithelial surface (Figure 12). In this schema, these 2 flagellated, NEU-deficient prokaryotes present their flagellin protein to the membrane-tethered mucin, MUC1, which in turn, recruits the eukaryotic sialidase, NEU1. NEU1-mediated MUC1-ED desialylation unmasks cryptic binding site(s) within its tandem repeats, rendering the MUC1-ED

hyperadhesive for these 2 bacteria. The rapid, extensive removal of numerous sialic acid molecules from the MUC1-ED generates conformational stress within its SEA domain, catalyzing autoproteolysis at its Gly-Ser cleavage site, generating the still hyperadhesive, flagellin-targeting MUC1-ED decoy receptor. This decoy receptor disrupts multiple flagellin-driven bacterial and host processes. Whether these findings can be extrapolated to (1) other flagellated, NEU-deficient respiratory pathogens, (2) extrapulmonary mucosal surfaces, (3) membrane-tethered mucins other than MUC1, (4) other sialylated receptors and surface-expressed sialoproteins, (5) other host sialidases, (6) prokaryotic neuraminidases, and/or (7) sialic acid-rich biofilm formation, requires further studies. Finally, our data establish the MUC1-ED decoy receptor as a mechanistically novel host response that may be harnessed as a therapeutic intervention to target select flagellated pathogens, including MDR strains.

Limitations of the study

In vitro studies using human airway epithelial cells were mostly performed using A549 cells derived from a lung adenocarcinoma. We only tested one strain each of WT Sm and Sm ΔFliC1,2,3 bacteria. The mechanism(s) whereby intracellular NEU1 desialylates the extracellular MUC1-ED was not determined. Two of the 4 known mammalian NEUs, NEU2 and NEU4, were not evaluated. Disease scores of Sm-infected mice were not measured as a means to determine whether WT Sm might cause more inflammation compared to flagellin-null Sm ΔFliC1,2,3. Other than promoting survival following lethal Sm challenge, we did not test whether rMUC1-ED might also exhibit other flagellin-targeting decoy receptor functions *in vivo*.

RESOURCE AVAILABILITY

Lead contact

Further information and requests for resources and reagents should be directed to and will be fulfilled by the lead contact, Erik Lillehoj (elillehoj@gmail.com).

Materials availability

This study generated 4 new reagents, the Sm FliC1,2,3 flagellin mixture and the purified Sm FliC1, Sm FliC2, and Sm FliC3 flagellins. These reagents are available from the lead contact upon request.

Data and code availability

- All data reported in this paper will be shared by the lead contact upon request.
- This paper does not report original code.
- Any additional information required to reanalyze the data reported in this paper is available from the lead contact upon request.

ACKNOWLEDGMENTS

We thank Dr. Inkyung Park for ANOVA, Dr. Stephanie Vogel and Dr. Alan Cross for critical review, and Ms. Shirley Taylor for secretarial support. This work was supported by grant AI-144497 from the U.S. National Institutes of Health (E.P.L.) and grant E01-W81XWH1910056 from the U.S. Department of Defense (E.P.L.).

AUTHOR CONTRIBUTIONS

E.P.L. and S.E.G. conceptualized the project. E.P.L. obtained IACUC and IRB approval. E.P.L. obtained funding. E.P.L., Y.Y., A.C.V., and A.I. performed the experiments. E.P.L., Y.Y., K.H.P., and S.E.G. performed data analysis. E.P.L., K.H.P., and S.E.G. wrote and revised the manuscript. K.H.P., H.I., and S.E.G. supervised the project. All authors read and approved the manuscript.

DECLARATION OF INTERESTS

The authors declare no competing interests.

STAR★METHODS

Detailed methods are provided in the online version of this paper and include the following:

- KEY RESOURCES TABLE
- EXPERIMENTAL MODEL AND STUDY PARTICIPANT DETAILS
  - Bacteria
  - Cell cultures
  - Murine model of Sm-Provoked MUC1-ED shedding
  - BAL in patients with ventilator-associated pneumonia
- METHOD DETAILS
  - Sm Adhesion to human airway epithelia
  - Sm Adhesion to plastics
  - Purification of Sm flagellins
  - SDS-PAGE and immunoblot assays
  - Sm motility assay
  - Fluorometric Sm flagellin binding assays
  - Flagellin structural analyses
  - Adenoviral constructs
  - Manipulation of MUC1, TLR5, and NEU1 expression
  - Expression and purification of human rMUC1-ED and its deletion mutants

SUPPLEMENTAL INFORMATION

Supplemental information can be found online at https://doi.org/10.1016/j.isci.2024.110866.

Received: April 10, 2024
Revised: August 3, 2024
Accepted: August 29, 2024
Published: August 31, 2024

REFERENCES

1. Hattrup, C.L., and Gendler, S.J. (2008). Structure and function of the cell surface (tethered) mucins. Annu. Rev. Physiol. *70*, 431–457. https://doi.org/10.1146/annurev.physiol.70.113006.100659.3.
2. Lillehoj, E.P., Kato, K., Lu, W., and Kim, K.C. (2013). Cellular and molecular biology of airway mucins. Int. Rev. Cell Mol. Biol. *303*, 139–202. https://doi.org/10.1016/B978-0-12-407697-6.00004-0.
3. Macao, B., Johansson, D.G.A., Hansson, G.C., and Härd, T. (2006). Autoproteolysis coupled to protein folding in the SEA domain of the membrane-bound MUC1 mucin. Nat. Struct. Mol. Biol. *13*, 71–76. https://doi.org/10.1038/nsmb1035.
4. Sandberg, A., Johansson, D.G.A., Macao, B., and Härd, T. (2008). SEA domain autoproteolysis accelerated by conformational strain: Energetic aspects. J. Mol. Biol. *377*, 1117–1129. https://doi.org/10.1016/j.jmb.2008.01.051.
5. Johansson, D.G.A., Macao, B., Sandberg, A., and Härd, T. (2008). SEA domain autoproteolysis accelerated by conformational strain: Mechanistic aspects. J. Mol. Biol. *377*, 1130–1143. https://doi.org/10.1016/j.jmb.2008.01.050.
6. Johansson, D.G.A., Wallin, G., Sandberg, A., Macao, B., Aqvist, J., and Härd, T. (2009). Protein autoproteolysis: conformational strain linked to the rate of peptide cleavage by the pH dependence of the N → O acyl shift reaction. J. Am. Chem. Soc. *131*, 9475–9477. https://doi.org/10.1021/ja9010817.
7. Hilkens, J., Ligtenberg, M.J., Vos, H.L., and Litvinov, S.V. (1992). Cell membrane-associated mucins and their adhesion-modulating property. Trends Biochem. Sci. *17*, 359–363. https://doi.org/10.1016/0968-0004(92)90315-z.
8. Lillehoj, E.P., Hyun, S.W., Kim, B.T., Zhang, X.G., Lee, D.I., Rowland, S., and Kim, K.C. (2001). Muc1 mucins on the cell surface are adhesion sites for *Pseudomonas aeruginosa*. Am. J. Physiol. Lung Cell Mol. Physiol. *280*, L181–L187. https://doi.org/10.1152/ajplung.2001.280.1.L181.
9. Lindén, S., Mahdavi, J., Hedenbro, J., Borén, T., and Carlstedt, I. (2004). Effects of pH on *Helicobacter pylori* binding to human gastric mucins: identification of binding to non-MUC5AC mucins. Biochem. J. *384*, 263–270. https://doi.org/10.1042/BJ20040402.
10. McAuley, J.L., Linden, S.K., Png, C.W., King, R.M., Pennington, H.L., Gendler, S.J., Florin, T.H., Hill, G.R., Korolik, V., and McGuckin, M.A. (2007). MUC1 cell surface mucin is a critical element of the mucosal barrier to infection. J. Clin. Invest. *117*, 2313–2324. https://doi.org/10.1172/JCI26705.
11. Parker, P., Sando, L., Pearson, R., Kongsuwan, K., Tellam, R.L., and Smith, S. (2010). Bovine Muc1 inhibits binding of enteric bacteria to Caco-2 cells. Glycoconj. J. *27*, 89–97. https://doi.org/10.1007/s10719-009-9269-2.
12. Xu, S., Peng, Z., Cui, B., Wang, T., Song, Y., Zhang, L., Wei, G., Wang, Y., and Shen, X. (2014). FliS modulates FlgM activity by acting as a non-canonical chaperone to control late flagellar gene expression, motility and biofilm formation in *Yersinia pseudotuberculosis*. Environ. Microbiol. *16*, 1090–1104. https://doi.org/10.1111/1462-2920.12222.
13. Müller, S., Alving, K., Peter-Katalinic, J., Zachara, N., Gooley, A.A., and Hanisch, F.G. (1999). High density O-glycosylation on tandem repeat peptide from secretory MUC1 of T47D breast cancer cells. J. Biol. Chem. *274*, 18165–18172. https://doi.org/10.1074/jbc.274.26.18165.
14. Ramos, H.C., Rumbo, M., and Sirard, J.C. (2004). Bacterial flagellins: mediators of pathogenicity and host immune responses in mucosa. Trends Microbiol. *12*, 509–517. https://doi.org/10.1016/j.tim.2004.09.002.
15. Akahoshi, D.T., and Bevins, C.L. (2022). Flagella at the host-microbe interface: Key functions intersect with redundant responses. Front. Immunol. *13*, 828758. https://doi.org/10.3389/fimmu.2022.828758.
16. Beachey, E.H. (1981). Bacterial adherence: adhesin-receptor interactions mediating the attachment of bacteria to mucosal surface. J. Infect. Dis. *143*, 325–345. https://doi.org/10.1093/infdis/143.3.325.
17. Zgair, A.K., and Chhibber, S. (2011). Adhesion of *Stenotrophomonas maltophilia* to mouse tracheal mucus is mediated through flagella. J. Med. Microbiol. *60*, 1032–1037. https://doi.org/10.1099/jmm.0.026377-0.
18. Pompilio, A., Crocetta, V., Confalone, P., Nicoletti, M., Petrucca, A., Guarnieri, S., Fiscarelli, E., Savini, V., Piccolomini, R., and Di Bonaventura, G. (2010). Adhesion to and biofilm formation on IB3-1 bronchial cells by *Stenotrophomonas maltophilia* isolates from cystic fibrosis patients. BMC Microbiol. *10*, 102. https://doi.org/10.1186/1471-2180-10-102.
19. Hajam, I.A., Dar, P.A., Shahnawaz, I., Jaume, J.C., and Lee, J.H. (2017). Bacterial flagellin-a potent immunomodulatory agent. Exp. Mol. Med. *49*, e373. https://doi.org/10.1038/emm.2017.172.
20. Wu, C.M., Huang, H.H., Li, L.H., Lin, Y.T., and Yang, T.C. (2022). Molecular characterization of three tandemly located flagellin genes of *Stenotrophomonas maltophilia*. Int. J. Mol. Sci. *23*, 3863. https://doi.org/10.3390/ijms23073863.
21. Lillehoj, E.P., Hyun, S.W., Liu, A., Guang, W., Verceles, A.C., Luzina, I.G., Atamas, S.P., Kim, K.C., and Goldblum, S.E. (2015). NEU1 sialidase regulates membrane-tethered mucin (MUC1) ectodomain adhesiveness for *Pseudomonas aeruginosa* and decoy receptor release. J. Biol. Chem. *290*, 18316–18331. https://doi.org/10.1074/jbc.M115.657114.
22. Lillehoj, E.P., Guang, W., Hyun, S.W., Liu, A., Hegerle, N., Simon, R., Cross, A.S., Ishida, H., Luzina, I.G., Atamas, S.P., and Goldblum, S.E. (2019). Neuraminidase 1-mediated desialylation of the mucin 1 ectodomain releases a decoy receptor that protects against *Pseudomonas aeruginosa* lung infection. J. Biol. Chem. *294*, 662–678. https://doi.org/10.1074/jbc.RA118.006022.
23. Verceles, A.C., Bhat, P., Nagaria, Z., Martin, D., Patel, H., Ntem-Mensah, A., Hyun, S.W., Hahn, A., Jeudy, J., Cross, A.S., et al. (2021). MUC1 ectodomain is a flagellin-targeting decoy receptor and biomarker operative during *Pseudomonas aeruginosa* lung infection. Sci. Rep. *11*, 22725. https://doi.org/10.1038/s41598-021-02242-x.
24. Xu, G., Ryan, C., Kiefel, M.J., Wilson, J.C., and Taylor, G.L. (2009). Structural studies on the *Pseudomonas aeruginosa* sialidase-like enzyme PA2794 suggest substrate and mechanistic variations. J. Mol. Biol. *386*, 828–840. https://doi.org/10.1016/j.jmb.2008.12.084.

25. d'Azzo, A., and Bonten, E. (2010). Molecular mechanisms of pathogenesis in a glycosphingolipid and a glycoprotein storage disease. Biochem. Soc. Trans. *38*, 1453–1457. https://doi.org/10.1042/BST0381453.
26. Bonten, E., van der Spoel, A., Fornerod, M., Grosveld, G., and d'Azzo, A. (1996). Characterization of human lysosomal neuraminidase defines the molecular basis of the metabolic storage disorder sialidosis. Genes Dev. *10*, 3156–3169. https://doi.org/10.1101/gad.10.24.3156.
27. Lukong, K.E., Elsliger, M.A., Chang, Y., Richard, C., Thomas, G., Carey, W., Tylki-Szymanska, A., Czartoryska, B., Buchholz, T., Criado, G.R., et al. (2000). Characterization of the sialidase molecular defects in sialidosis patients suggests the structural organization of the lysosomal multienzyme complex. Hum. Mol. Genet. *9*, 1075–1085. https://doi.org/10.1093/hmg/9.7.1075.
28. D'Avila, F., Tringali, C., Papini, N., Anastasia, L., Croci, G., Massaccesi, L., Monti, E., Tettamanti, G., and Venerando, B. (2013). Identification of lysosomal sialidase NEU1 and plasma membrane sialidase NEU3 in human erythrocytes. J. Cell. Biochem. *114*, 204–211. https://doi.org/10.1002/jcb.24355.
29. Pshezhetsky, A.V., and Ashmarina, L.I. (2013). Desialylation of surface receptors as a new dimension in cell signaling. Biochemistry. *78*, 736–745. https://doi.org/10.1134/S0006297913070067.
30. Lillehoj, E.P., Hyun, S.W., Feng, C., Zhang, L., Liu, A., Guang, W., Nguyen, C., Luzina, I.G., Atamas, S.P., Passaniti, A., et al. (2012). NEU1 sialidase expressed in human airway epithelia regulates epidermal growth factor receptor (EGFR) and MUC1 protein signaling. J. Biol. Chem. *287*, 8214–8231. https://doi.org/10.1074/jbc.M111.292888.
31. Majumdar, R., Karthikeyan, H., Senthilnathan, V., and Sugumar, S. (2022). Review on *Stenotrophomonas maltophilia*: An emerging multidrug-resistant opportunistic pathogen. Recent Pat. Biotechnol. *16*, 329–354. https://doi.org/10.2174/1872208316666220512121205.
32. Brooke, J.S. (2021). Advances in the microbiology of *Stenotrophomonas maltophilia*. Clin. Microbiol. Rev. *34*, e0003019. https://doi.org/10.1128/CMR.00030-19.
33. Fujita, J., Yamadori, I., Xu, G., Hojo, S., Negayama, K., Miyawaki, H., Yamaji, Y., and Takahara, J. (1996). Clinical features of *Stenotrophomonas maltophilia* pneumonia in immunocompromised patients. Respir. Med. *90*, 35–38. https://doi.org/10.1016/s0954-6111(96)90242-5.
34. Brooke, J.S., Di Bonaventura, G., Berg, G., and Martinez, J.L. (2017). Editorial: A multidisciplinary look at *Stenotrophomonas maltophilia*: An emerging multi-drug-resistant global opportunistic pathogen. Front. Microbiol. *8*, 1511. https://doi.org/10.3389/fmicb.2017.01511.
35. Ramos-Hegazy, L., Chakravarty, S., and Anderson, G.G. (2020). Phosphoglycerate mutase affects *Stenotrophomonas maltophilia* attachment to biotic and abiotic surfaces. Microbes Infect. *22*, 60–64. https://doi.org/10.1016/j.micinf.2019.08.001.
36. Mandell, G.L., Bennett, J.E., and Dolin, R. (2010). Mandell, Douglas and Bennett's Principles and Practice of Infectious Diseases (Elsevier).
37. de Oliveira-Garcia, D., Dall'Agnol, M., Rosales, M., Azzuz, A.C.G.S., Alcántara, N., Martinez, M.B., and Girón, J.A. (2003). Fimbriae and adherence of *Stenotrophomonas maltophilia* to epithelial cells and to abiotic surfaces. Cell Microbiol. *5*, 625–636. https://doi.org/10.1046/j.1462-5822.2003.00306.x.
38. Hayashi, F., Smith, K.D., Ozinsky, A., Hawn, T.R., Yi, E.C., Goodlett, D.R., Eng, J.K., Akira, S., Underhill, D.M., and Aderem, A. (2001). The innate immune response to bacterial flagellin is mediated by Toll-like receptor 5. Nature *410*, 1099–1103. https://doi.org/10.1038/35074106.
39. Lillehoj, E.P., Kim, B.T., and Kim, K.C. (2002). Identification of *Pseudomonas aeruginosa* flagellin as an adhesin for Muc1 mucin. Am. J. Physiol. Lung Cell Mol. Physiol. *282*, L751–L756. https://doi.org/10.1152/ajplung.00383.2001.
40. Kato, K., Lillehoj, E.P., Park, Y.S., Umehara, T., Hoffman, N.E., Madesh, M., and Kim, K.C. (2012). Membrane-tethered MUC1 mucin is phosphorylated by epidermal growth factor receptor in airway epithelial cells and associates with TLR5 to inhibit recruitment of MyD88. J. Immunol. *188*, 2014–2022. https://doi.org/10.4049/jimmunol.1102405.
41. Kato, K., Lillehoj, E.P., Kai, H., and Kim, K.C. (2010). MUC1 expression by human airway epithelial cells mediates *Pseudomonas aeruginosa* adhesion. Front. Biosci. *2*, 68–77. https://doi.org/10.2741/e67.
42. Lillehoj, E.P., Kim, H., Chun, E.Y., and Kim, K.C. (2004). *Pseudomonas aeruginosa* stimulates phosphorylation of the airway epithelial membrane glycoprotein Muc1 and activates MAP kinase. Am. J. Physiol. Lung Cell Mol. Physiol. *287*, L809–L815. https://doi.org/10.1152/ajplung.00385.2003.
43. Hyun, S.W., Liu, A., Liu, Z., Cross, A.S., Verceles, A.C., Magesh, S., Kommagalla, Y., Kona, C., Ando, H., Luzina, I.G., et al. (2016). The NEU1-selective sialidase inhibitor, C9-butyl-amide-DANA, blocks sialidase activity and NEU1-mediated bioactivities in human lung *in vitro* and murine lung *in vivo*. Glycobiology *26*, 834–849. https://doi.org/10.1093/glycob/cww060.
44. Lee, C., Liu, A., Miranda-Ribera, A., Hyun, S.W., Lillehoj, E.P., Cross, A.S., Passaniti, A., Grimm, P.R., Kim, B.Y., Welling, P.A., et al. (2014). NEU1 sialidase regulates the sialylation state of CD31 and disrupts CD31-driven capillary-like tube formation in human lung microvascular endothelia. J. Biol. Chem. *289*, 9121–9135. https://doi.org/10.1074/jbc.M114.555888.
45. Storr, S.J., Royle, L., Chapman, C.J., Hamid, U.M.A., Robertson, J.F., Murray, A., Dwek, R.A., and Rudd, P.M. (2008). The O-linked glycosylation of secretory/shed MUC1 from an advanced breast cancer patient's serum. Glycobiology *18*, 456–462. https://doi.org/10.1093/glycob/cwn022.
46. Remold-O'Donnell, E., and Rosen, F.S. (1990). Proteolytic fragmentation of sialophorin (CD43). Localization of the activation-inducing site and examination of the role of sialic acid. J. Immunol. *145*, 3372–3378.
47. Ward, S., O'Sullivan, J.M., and O'Donnell, J.S. (2019). von Willebrand factor sialylation-A critical regulator of biological function. J. Thromb. Haemost. *17*, 1018–1029. https://doi.org/10.1111/jth.14471.
48. Thathiah, A., Blobel, C.P., and Carson, D.D. (2003). Tumor necrosis factor-α converting enzyme/ADAM 17 mediates MUC1 shedding. J. Biol. Chem. *278*, 3386–3394. https://doi.org/10.1074/jbc.M208326200.
49. Thathiah, A., and Carson, D.D. (2004). MT1-MMP mediates MUC1 shedding independent of TACE/ADAM17. Biochem. J. *382*, 363–373. https://doi.org/10.1042/BJ20040513.
50. Julian, J., Dharmaraj, N., and Carson, D.D. (2009). MUC1 is a substrate for γ-secretase. J. Cell. Biochem. *108*, 802–815. https://doi.org/10.1002/jcb.22292.
51. Nedeljković, M., Sastre, D.E., and Sundberg, E.J. (2021). Bacterial flagellar filament: A supramolecular multifunctional nanostructure. Int. J. Mol. Sci. *22*, 7521. https://doi.org/10.3390/ijms22147521.
52. Kim, K.C., Wasano, K., Niles, R.M., Schuster, J.E., Stone, P.J., and Brody, J.S. (1987). Human neutrophil elastase releases cell surface mucins from primary cultures of hamster tracheal epithelial cells. Proc. Natl. Acad. Sci. USA *84*, 9304–9308. https://doi.org/10.1073/pnas.84.24.9304.
53. Ohbayashi, H. (2005). Current synthetic inhibitors of human neutrophil elastase in 2005. Expert Opin. Ther. Pat. *15*, 759–771. https://doi.org/10.1517/13543776.15.7.759.
54. Hirota, Y., Suzuki, M., Yamaguchi, K., Fujita, T., and Katsube, N. (2004). Effects of the neutrophil elastase inhibitor (ONO-6818) on acetic acid induced colitis in Syrian hamsters. J. Vet. Med. Sci. *66*, 1223–1228. https://doi.org/10.1292/jvms.66.1223.
55. Fray, M.J., Dickinson, R.P., Huggins, J.P., and Occleston, N.L. (2003). A potent, selective inhibitor of matrix metalloproteinase-3 for the topical treatment of chronic dermal ulcers. J. Med. Chem. *46*, 3514–3525. https://doi.org/10.1021/jm0308038.
56. Chan, Z.C.K., Kwan, H.L.R., Wong, Y.S., Jiang, Z., Zhou, Z., Tam, K.W., Chan, Y.S., Chan, C.B., and Lee, C.W. (2020). Site-directed MT1-MMP trafficking and surface insertion regulate AChR clustering and remodeling at developing NMJs. Elife *9*, e54379. https://doi.org/10.7554/eLife.54379.
57. Martone, R.L., Zhou, H., Atchison, K., Comery, T., Xu, J.Z., Huang, X., Gong, X., Jin, M., Kreft, A., Harrison, B., et al. (2009). Begacestat (GSI-953): A novel, selective thiophene sulfonamide inhibitor of amyloid precursor protein γ-secretase for the treatment of Alzheimer's disease. J. Pharmacol. Exp. Ther. *331*, 598–608. https://doi.org/10.1124/jpet.109.152975.
58. McCaw, T.R., Inga, E., Chen, H., Jaskula-Sztul, R., Dudeja, V., Bibb, J.A., Ren, B., and Rose, J.B. (2021). Gamma secretase inhibitors in cancer: A current perspective on clinical performance. Oncol. *26*, e608–e621. https://doi.org/10.1002/onco.13627.
59. Lillehoj, E.P., Han, F., and Kim, K.C. (2003). Mutagenesis of a Gly-Ser cleavage site in MUC1 inhibits ectodomain shedding. Biochem. Biophys. Res. Commun. *307*, 743–749. https://doi.org/10.1016/s0006-291x(03)01260-9.
60. Prince, A. (1992). Adhesins and receptors of *Pseudomonas aeruginosa* associated with infection of the respiratory tract. Microb. Pathog. *13*, 251–260. https://doi.org/10.1016/0882-4010(92)90035-m.
61. Fontenot, J.D., Mariappan, S.V., Catasti, P., Domenech, N., Finn, O.J., and Gupta, G.

(1995). Structure of a tumor associated antigen containing a tandemly repeated immunodominant epitope. J. Biomol. Struct. Dyn. *13*, 245–260. https://doi.org/10.1080/07391102.1995.10508837.
62. Agrawal, B., Krantz, M.J., Reddish, M.A., and Longenecker, B.M. (1998). Cancer-associated MUC1 mucin inhibits human T-cell proliferation, which is reversible by IL-2. Nat. Med. *4*, 43–49. https://doi.org/10.1038/nm0198-043.
63. Kam, J.L., Regimbald, L.H., Hilgers, J.H., Hoffman, P., Krantz, M.J., Longenecker, B.M., and Hugh, J.C. (1998). MUC1 synthetic peptide inhibition of intercellular adhesion molecule-1 and MUC1 binding requires six tandem repeats. Cancer Res. *58*, 5577–5581.
64. Zgair, A.K., and Chhibber, S. (2011). Immunoassay method to check the flagellin mediated binding of *Stenotrophomonas maltophilia* to polystyrene. Mikrobiologiia *80*, 136–138.
65. Pompilio, A., Piccolomini, R., Picciani, C., D'Antonio, D., Savini, V., and Di Bonaventura, G. (2008). Factors associated with adherence to and biofilm formation on polystyrene by *Stenotrophomonas maltophilia*: The role of cell surface hydrophobicity and motility. FEMS Microbiol. Lett. *287*, 41–47. https://doi.org/10.1111/j.1574-6968.2008.01292.x.
66. Jucker, B.A., Harms, H., and Zehnder, A.J. (1996). Adhesion of the positively charged bacterium *Stenotrophomonas* (*Xanthomonas*) *maltophilia* 70401 to glass and Teflon. J. Bacteriol. *178*, 5472–5479. https://doi.org/10.1128/jb.178.18.5472-5479.1996.
67. Passerini de Rossi, B., Calenda, M., Vay, C., and Franco, M. (2007). Biofilm formation by *Stenotrophomonas maltophilia* isolates from device-associated nosocomial infections. Rev. Argent. Microbiol. *39*, 204–212.
68. Featherstone, P.J., Ball, C.M., and Westhorpe, R.N. (2015). The evolution of the polyvinyl chloride endotracheal tube. Anaesth. Intensive Care *43*, 435–436. https://doi.org/10.1177/0310057X1504300401.
69. Varki, N.M., and Varki, A. (2007). Diversity in cell surface sialic acid presentations: implications for biology and disease. Lab. Invest. *87*, 851–857. https://doi.org/10.1038/labinvest.3700656.
70. Schauer, R., and Kamerling, J.P. (2018). Exploration of the sialic acid world. Adv. Carbohydr. Chem. Biochem. *75*, 1–213. https://doi.org/10.1016/bs.accb.2018.09.001.33.
71. Lewis, A.L., and Lewis, W.G. (2012). Host sialoglycans and bacterial sialidases: a mucosal perspective. Cell Microbiol. *14*, 1174–1182. https://doi.org/10.1111/j.1462-5822.2012.01807.x.
72. Noguera, M.E., Jakoncic, J., and Ermácora, M.R. (2020). High-resolution structure of intramolecularly proteolyzed human mucin-1 SEA domain. Biochim. Biophys. Acta. Proteins Proteom. *1868*, 140361. https://doi.org/10.1016/j.bbapap.2020.140361.
73. Guillot, A., Dauchez, M., Belloy, N., Jonquet, J., Duca, L., Romier, B., Maurice, P., Debelle, L., Martiny, L., Durlach, V., et al. (2016). Impact of sialic acids on the molecular dynamic of bi-antennary and tri-antennary glycans. Sci. Rep. *6*, 35666. https://doi.org/10.1038/srep35666.
74. Yamaguchi, K., Shiozaki, K., Moriya, S., Koseki, K., Wada, T., Tateno, H., Sato, I., Asano, M., Iwakura, Y., and Miyagi, T. (2012). Reduced susceptibility to colitis-associated colon carcinogenesis in mice lacking plasma membrane-associated sialidase. PLoS One *7*, e41132. https://doi.org/10.1371/journal.pone.0041132.
75. Ohyashiki, T., Taka, M., and Mohri, T. (1989). Changes in the membrane surface charge density and/or membrane potential of the porcine intestinal brush-border membrane vesicles induced by treatment with neuraminidase. J. Biochem. *106*, 584–588. https://doi.org/10.1093/oxfordjournals.jbchem.a122899.
76. Siebert, H.C., André, S., Reuter, G., Kaptein, R., Vliegenthart, J.F., and Gabius, H.J. (1997). Comparison between intact and desialylated human serum amyloid P component by laser photo CIDNP (chemically induced dynamic nuclear polarization) technique: An indication for a conformational impact of sialic acid. Glycoconj. J. *14*, 945–949. https://doi.org/10.1023/a:1018570912192.
77. Paiva, M.M., Soeiro, M.N.C., Barbosa, H.S., Meirelles, M.N.L., Delain, E., and Araújo-Jorge, T.C. (2010). Glycosylation patterns of human α2-macroglobulin: Analysis of lectin binding by electron microscopy. Micron *41*, 666–673. https://doi.org/10.1016/j.micron.2010.02.015.
78. Pan, D., and Song, Y. (2010). Role of altered sialylation of the I-like domain of β1 integrin in the binding of fibronectin to β1 integrin: Thermodynamics and conformational analyses. Biophys. J. *99*, 208–217. https://doi.org/10.1016/j.bpj.2010.03.063.
79. Huang, R.Y.C., and Hudgens, J.W. (2013). Effects of desialylation on human α1-acid glycoprotein-ligand interactions. Biochemistry *52*, 7127–7136. https://doi.org/10.1021/bi4011094.
80. Baycin-Hizal, D., Gottschalk, A., Jacobson, E., Mai, S., Wolozny, D., Zhang, H., Krag, S.S., and Betenbaugh, M.J. (2014). Physiologic and pathophysiologic consequences of altered sialylation and glycosylation on ion channel function. Biochem. Biophys. Res. Commun. *453*, 243–253. https://doi.org/10.1016/j.bbrc.2014.06.067.
81. Wang, A.L., Zhou, Y., Palmieri, M.J., and Hao, G.G. (2018). Hydrogen deuterium exchange reveals changes to protein dynamics of recombinant human erythropoietin upon N- and O-desialylation. J. Pharm. Biomed. Anal. *154*, 454–459. https://doi.org/10.1016/j.jpba.2018.02.060.
82. Fougerat, A., Pan, X., Smutova, V., Heveker, N., Cairo, C.W., Issad, T., Larrivée, B., Medin, J.A., and Pshezhetsky, A.V. (2018). Neuraminidase 1 activates insulin receptor and reverses insulin resistance in obese mice. Mol. Metab. *12*, 76–88. https://doi.org/10.1016/j.molmet.2018.03.017.
83. Feng, C., Zhang, L., Almulki, L., Faez, S., Whitford, M., Hafezi-Moghadam, A., and Cross, A.S. (2011). Endogenous PMN sialidase activity exposes activation epitope on CD11b/CD18 which enhances its binding interaction with ICAM-1. J. Leukoc. Biol. *90*, 313–321. https://doi.org/10.1189/jlb.1210708.
84. Waters, V.J., Gómez, M.I., Soong, G., Amin, S., Ernst, R.K., and Prince, A. (2007). Immunostimulatory properties of the emerging pathogen *Stenotrophomonas maltophilia*. Infect. Immun. *75*, 1698–1703. https://doi.org/10.1128/IAI.01469-06.
85. Cross, A.S., Hyun, S.W., Miranda-Ribera, A., Feng, C., Liu, A., Nguyen, C., Zhang, L., Luzina, I.G., Atamas, S.P., Twaddell, W.S., et al. (2012). NEU1 and NEU3 sialidase activity expressed in human lung microvascular endothelia: NEU1 restrains endothelial cell migration, whereas NEU3 does not. J. Biol. Chem. *287*, 15966–15980. https://doi.org/10.1074/jbc.M112.346817.
86. Jumper, J., Evans, R., Pritzel, A., Green, T., Figurnov, M., Ronneberger, O., Tunyasuvunakool, K., Bates, R., Žídek, A., Potapenko, A., et al. (2021). Highly accurate protein structure prediction with AlphaFold. Nature *596*, 583–589. https://doi.org/10.1038/s41586-021-03819-2.
87. Baek, M., DiMaio, F., Anishchenko, I., Dauparas, J., Ovchinnikov, S., Lee, G.R., Wang, J., Cong, Q., Kinch, L.N., Schaeffer, R.D., et al. (2021). Accurate prediction of protein structures and interactions using a three-track neural network. Science *373*, 871–876. https://doi.org/10.1126/science.abj8754.
88. Pettersen, E.F., Goddard, T.D., Huang, C.C., Meng, E.C., Couch, G.S., Croll, T.I., Morris, J.H., and Ferrin, T.E. (2021). UCSF ChimeraX: Structure visualization for researchers, educators, and developers. Protein Sci. *30*, 70–82. https://doi.org/10.1002/pro.3943.
89. Hu, R.M., Huang, K.J., Wu, L.T., Hsiao, Y.J., and Yang, T.C. (2008). Induction of L1 and L2 β-lactamases of *Stenotrophomonas maltophilia*. Antimicrob. Agents Chemother. *52*, 1198–1200. https://doi.org/10.1128/AAC.00682-07.
90. Hyun, S.W., Anglin, I.E., Liu, A., Yang, S., Sorkin, J.D., Lillehoj, E., Tonks, N.K., Passaniti, A., and Goldblum, S.E. (2011). Diverse injurious stimuli reduce protein tyrosine phosphatase-μ expression and enhance epidermal growth factor receptor signaling in human airway epithelia. Exp. Lung Res. *37*, 327–343. https://doi.org/10.3109/01902148.2011.566673.
91. Kalil, A.C., Metersky, M.L., Klompas, M., Muscedere, J., Sweeney, D.A., Palmer, L.B., Napolitano, L.M., O'Grady, N.P., Bartlett, J.G., Carratalà, J., et al. (2016). Executive summary: Management of adults with hospital-acquired and ventilator-associated pneumonia: 2016 clinical practice guidelines by the Infectious Diseases Society of America and the American Thoracic Society. Clin. Infect. Dis. *63*, 575–582. https://doi.org/10.1093/cid/ciw504.
92. Clinical and Laboratory Standards Institute (CLSI) (2015). Performance Standards for Antimicrobial Susceptibility Testing. Twenty-Fifth Informational Supplement. CLSI Document M100-S25 (CSLI).
93. Guang, W., Ding, H., Czinn, S.J., Kim, K.C., Blanchard, T.G., and Lillehoj, E.P. (2010). Muc1 cell surface mucin attenuates epithelial inflammation in response to a common mucosal pathogen. J. Biol. Chem. *285*, 20547–20557. https://doi.org/10.1074/jbc.M110.121319.
94. Song, W.S., and Yoon, S.i. (2014). Crystal structure of FliC flagellin from *Pseudomonas aeruginosa* and its implication in TLR5 binding and formation of the flagellar filament. Biochem. Biophys. Res. Commun. *444*, 109–115. https://doi.org/10.1016/j.bbrc.2014.01.008.

95. Maki-Yonekura, S., Yonekura, K., and Namba, K. (2010). Conformational change of flagellin for polymorphic supercoiling of the flagellar filament. Nat. Struct. Mol. Biol. *17*, 417–422. https://doi.org/10.1038/nsmb.1774.

96. Nedeljković, M., Kreutzberger, M.A.B., Postel, S., Bonsor, D., Xing, Y., Jacob, N., Schuler, W.J., Egelman, E.H., and Sundberg, E.J. (2023). An unbroken network of interactions connecting flagellin domains is required for motility in viscous environments. PLoS Pathog. *19*, e1010979. https://doi.org/10.1371/journal.ppat.1010979.

97. Lillehoj, E.P., Hyun, S.W., Feng, C., Zhang, L., Liu, A., Guang, W., Nguyen, C., Sun, W., Luzina, I.G., Webb, T.J., et al. (2014). Human airway epithelia express catalytically active NEU3 sialidase. Am. J. Physiol. Lung Cell Mol. Physiol. *306*, L876–L886. https://doi.org/10.1152/ajplung.00322.2013.

98. Green, M.R., and Sambrook, J. (2012). Molecular Cloning. A Laboratory Manual, 4th edition (Cold Spring Harbor Laboratory Press).

99. Hyun, S.W., Imamura, A., Ishida, H., Piepenbrink, K.H., Goldblum, S.E., and Lillehoj, E.P. (2021). The sialidase NEU1 directly interacts with the juxtamembranous segment of the cytoplasmic domain of mucin-1 to inhibit downstream PI3K-Akt signaling. J. Biol. Chem. *297*, 101337. https://doi.org/10.1016/j.jbc.2021.101337.

100. Wu, W., Punt, J.A., Granger, L., Sharrow, S.O., and Kearse, K.P. (1997). Developmentally regulated expression of peanut agglutinin (PNA)-specific glycans on murine thymocytes. Glycobiology *7*, 349–356. https://doi.org/10.1093/glycob/7.3.349.

101. Machin, D., Campbell, M., Fayers, P., and Pinol, A. (1997). Sample Size Tables for Clinical Studies, 2nd edition (Blackwell Science).

102. Zar, J.H. (1984). Biostatistical Analysis, 2nd edition (Prentice-Hall).

STAR★METHODS

KEY RESOURCES TABLE

REAGENT or RESOURCE	SOURCE	IDENTIFIER
Antibodies		
Rabbit anti-mouse MUC1-ED	LifeSpan BioSciences	Cat# LS-C88106; RRID: AB_1809766
Mouse anti-human MUC1-ED	Thermo Fisher Scientific	Cat# MA1-06503; RRID: AB_558126
Hamster anti-human MUC1-CD	Thermo Fisher Scientific	Cat# MA5-11202; RRID: AB_11000874
Mouse anti-human IL-8	Thermo Fisher Scientific	Cat# M801; RRID: AB_223583
Mouse anti-human β-tubulin	Thermo Fisher Scientific	Cat# MA5-16308; RRID: AB_2537819
Rabbit anti-human NEU1	Abcam	Cat# ab1141807; RRID: AB_1141807
Rabbit anti-human PPCA	Abcam	Cat# ab126127; RRID: AB_11129908
Rabbit anti-human NEU3	Sigma-Aldrich	Cat# HPA038730; RRID: AB_2676180
Mouse anti-human TLR5	Santa Cruz Biotechnology	Cat# sc-52963; RRID: AB_793184
Mouse anti-human phospho-ERK1/2	BD Biosciences	Cat# 612358; RRID:AB_399647
Mouse anti-human ERK2	BD Biosciences	Cat# 610103; RRID: AB_397509
HRP-conjugated rabbit anti-mouse IgG	KPL	Cat# 61-6520; RRID: AB_2533933
HRP-conjugated goat anti-rabbit IgG	KPL	Cat# 65-6120; RRID: AB_2533967
HRP-conjugated goat anti-hamster IgG	KPL	Cat# PA1-29626; RRID: AB_10985385
Bacterial and virus strains		
Stenotrophomonas maltophilia strain KJ	Wu et al.[20]	N/A
Stenotrophomonas maltophilia strain KJ ΔFliC1,2,3	Wu et al.[20]	N/A
E. coli NEB 5-alpha	New England Biolabs	Cat# C2987H
Biological samples		
Sm FliC1,2,3 flagellin mixture	This study	N/A
Sm FliC1 flagellin	This study	N/A
Sm FliC2 flagellin	This study	N/A
Sm FliC3 flagellin	This study	N/A
Patient-derived BALF	Verceles et al.[23]	N/A
Chemicals, peptides, and recombinant proteins		
C9-BA-DANA	Hyun et al.[43]	N/A
4-MU-NANA	Sigma-Aldrich	Cat# 69587
Asialofetuin	Sigma-Aldrich	Cat# F3004
Fetuin	Sigma-Aldrich	Cat# A4781
Critical commercial assays		
Vitek MS	bioMerieux	Ver.3.2
Experimental models: Cell lines		
A549	ATCC	Cat# CRM-CCL-185
HEK293T	ATCC	Cat# CRL-3216
1HAEo$^-$	Laboratory of Dieter Gruenert, California Pacific Medical Center Research Institute	N/A
CFTE29o	Laboratory of Dieter Gruenert, California Pacific Medical Center Research Institute	N/A

(*Continued on next page*)

Continued

REAGENT or RESOURCE	SOURCE	IDENTIFIER
16HBE14o-	Laboratory of Dieter Gruenert, California Pacific Medical Center Research Institute	N/A
BEAS-2B	Laboratory of Sekhar Reddy, University of Illinois Cancer Center	N/A
SAEC	Lonza	Cat# CC-2547
Experimental models: Organisms/strains		
Mouse: DBA/2J	The Jackson Laboratory	RRID:IMSR_JAX:000671
Oligonucleotides		
NEU1 siRNA	Dharmacon	Cat # L-011092-00-0005
NEU3 siRNA	Dharmacon	Cat # L-010641-02-0005
MUC1 siRNA	Dharmacon	Cat# # M-004019-02-0020
Nontargeting control siRNA	Dharmacon	Cat # D-001810-01-05
Recombinant DNA		
pcDNA3.1(+)	Thermo Fisher Scientific	Cat# V79020
pBAD/His-B	Thermo Fisher Scientific	Cat# V43001
pTLR5	Laboratory of Stephanie Vogel, University of Maryland	N/A
Ad-MUC1	GenScript	Custom synthesis
Ad-GFP	GenScript	Custom synthesis
Ad-NEU1	Cross et al.[85]	N/A
Ad-NEU1-G68V	Cross et al.[85]	N/A
Ad-NEU3	Cross et al.[85]	N/A
MUC1-ED-WT, aal-375	Lillehoj et al.[59]	N/A
MUC1-ED-Δ1, aal-311	GenScript	Custom synthesis
MUC1-ED-Δ2, aa312-375	GenScript	Custom synthesis
MUC1-ED-Δ3, aa 1-131	GenScript	Custom synthesis
MUC1-ED-Δ4, aa 1-71	GenScript	Custom synthesis
MUC1-ED-Δ5, aa 1-31	GenScript	Custom synthesis
Software and algorithms		
SAS software	SAS Institute	Ver. 9.4
Excel	Microsoft	Windows 11
Mantel-Cox log rank test	https://www.evanmiller.org/ab-testing/survival-curves.html	N/A
AlphaFold2	Jumper et al.[86]	N/A
RoseTTAFold	Baek et al.[87]	N/A
UCSF ChimeraX	Pettersen et al.[88]	N/A
ImageJ	https://imagej.net/ij/	N/A
Other		
Ni-NTA-agarose	Thermo Fisher Scientific	Cat# R90101
Protein G agarose	Thermo Fisher Scientific	Cat# 20397
Biotinylated PNA	Vector Laboratories	Cat# B-1075-5
PNA-agarose	Vector Laboratories	Cat# AL-1073
Lipofectamine 2000	Invitrogen	Cat# 11668030
HRP-conjugated streptavidin	Sigma-Aldrich	Cat# RABHRP3
Polymyxin B-agarose	Sigma-Aldrich	Cat# P1411

(*Continued on next page*)

Continued

REAGENT or RESOURCE	SOURCE	IDENTIFIER
Macro-Prep High Q	Bio-Rad	Cat# 1580040
Endotracheal tube	Serfinity Medical	Cat# 1010156
Human MUC1 ELISA	Lillehoj et al.[22]	N/A
Mouse MUC1 ELISA	Lillehoj et al.[22]	N/A

EXPERIMENTAL MODEL AND STUDY PARTICIPANT DETAILS

Bacteria

The parental Sm strain KJ expressing FliC1, FliC2, and FliC3 flagellins and the flagellin-null Sm ΔFliC1,2,3 bacterial strain were kindly provided by Dr. Tsuey-Ching Yang, Department of Biotechnology, Laboratory Science in Medicine, National Yang Ming Chiao Tung University, Taipei, Taiwan.[20] The parental KJ strain is a Sm clinical isolate.[89] Bacteria were cultured at 37°C in LB medium (10 mg/mL tryptone, 5.0 mg/mL yeast abstract, 10 mg/mL NaCl) (Thermo Fisher Scientific, Waltham, MA), and quantified spectrophotometrically at A_{600}.

Cell cultures

Human airway ECs derived from distinct regions of the airway, including the trachea (1HAEo$^-$ and CFTE29o$^-$ cells), bronchus (16HBE14o$^-$ and BEAS-2B cells), terminal bronchioles (small airway epithelial cells [SAECs]), and alveolus (A549 cells) were studied. The sex of these cells has not been reported and the cell lines were not authenticated or tested for mycoplasma contamination. A549 cells are an alveolar type II cell line derived from a lung adenocarcinoma (American Type Culture Collection, Manassas, VA). 16HBE14o$^-$, CFTE29o$^-$, and 1HAEo$^-$ are SV40 T antigen transformed cell lines that were provided by Dr. Dieter Gruenert (California Pacific Medical Center Research Institute, San Francisco, CA). BEAS-2B is an SV40-transformed cell line that was provided by Dr. Sekhar Reddy (University of Illinois, Chicago, IL). HEK293T cells were from ATCC. Cells were cultured at 37°C in 5% CO_2 in Dulbecco's modified Eagle's medium (Invitrogen, Carlsbad, CA) containing 10% fetal bovine serum (Hyclone Laboratories, Logan, UT), 50 units/ml penicillin, and 50 μg/mL streptomycin. Human primary SAECs (Lonza, Walkersville, MD) were cultured at 37°C in 5% CO_2 in predefined small airway growth medium (Lonza) containing hydrocortisone, human EGF, epinephrine, transferrin, insulin, retinoic acid, triiodothyronine, and fatty acid-free bovine serum albumin.[90] Only SAEC passages 2–4 were studied.

Murine model of Sm-Provoked MUC1-ED shedding

Animal studies were reviewed and approved by the University of Maryland Baltimore Institutional Animal Use and Care Committee (protocol number 0617005) and conducted in accordance with guidelines of the Care and Use of Laboratory Animals of the National Institutes of Health. Equal numbers of male and female adult DBA/2 mice (18–20 g, 20–22 weeks) (The Jackson Laboratory, Bar Harbor, ME) were randomly assigned to the experimental groups and administered i.n. with 1.0×10^8 CFU/mouse of the flagellin-expressing WT Sm strain, the flagellin-null Sm strain, or PBS control. In other experiments, mice were administered i.n. with 10 ng/mouse of the purified, LPS-free, Sm FliC1,2,3 flagellin mixture or PBS control. In still other experiments, mice were administered i.p. with 170 nmol/g (15 ng/g) body weight of C9-BA-DANA or PBS control. After 24 h, mice were administered i.p. with a second identical dose of the same inhibitor or PBS control and administered i.n. with 100 ng/mouse of the Sm FliC1,2,3 flagellin mixture. After an additional 24 h, the mice were euthanized by CO_2 inhalation and cervical dislocation, and BALF harvested. Pyrogen-free 0.9% NaCl was introduced i.t. into the lungs in 5 x 1.0-mL aliquots, after which the BALF was retrieved with gentle suction, its volume recorded, and samples placed on ice. The BALF was filtered through sterile gauze, centrifuged at 450xg to remove cells, and the supernatants concentrated 25-fold by passage through membrane filters (pore size 10 kDa) mounted in Centricon tubes (Millipore, Burlington, MA). BALF samples were assayed for shed MUC1-ED levels by ELISA and normalized to total protein concentration. In mouse survival studies, male and female DBA/2 mice were administered i.n. with increasing inocula ($1x10^9$-$1x10^{11}$ CFU) of Sm and survival measured daily by Kaplan-Meier analysis.[22] In other survival studies, mice were co-administered i.n. with 1×10^{11} CFU of Sm plus 100 μg/g body weight of human rMUC1-ED-WT or PBS control and survival measured.

BAL in patients with ventilator-associated pneumonia

This study was conducted in accordance with the Declaration of Helsinki and other local statutes or regulations protecting subjects in biomedical research, and was approved by the Institutional Review Board of the University of Maryland Baltimore (protocol numbers HP-00059183 and HP-00083805). The age, sex, gender, ancestry, race, ethnicity, and socioeconomic status of the participants has been reported.[23] Informed consent was obtained from all participants. BAL was performed on patients diagnosed with ventilator-associated pneumonia. Clinical diagnosis of pneumonia was based on findings of a new infiltrate by chest X-ray or CAT scan in the setting of fever, purulent sputum, leukocytosis, and diminished oxygenation.[91] Briefly, after conscious sedation with fentanyl and midazolam, and local anesthesia with 2% lidocaine, the bronchoscope was wedged in a 3rd or 4th order bronchus, after which 125 mL of sterile pyrogen-free 0.9% NaC1 was injected in 25-mL aliquots and the BALF retrieved and pooled. An aliquot of BALF was cultured and bacteria identified at the University of Maryland Medical Center Clinical Microbiology Laboratory following standard laboratory procedures using the Vitek MS automated mass spectrometry

microbial identification system (Biomerieux, Marcy l'Etoile, France) and interpreted according to clinical and Laboratory Standards Institute criteria.[92] The remainder of the BALF was filtered through sterile gauze, centrifuged at 450xg to remove cells, and the supernatant concentrated 25-fold by ultrafiltration and stored at −80°C until use. Studies on the BALF included quantitation of MUC1-ED by ELISA and a total protein assay. VAP patients culture-positive for only Sm, bacteria other than Sm (*E. coli*, *P. mirabilis*, *K. pneumoniae*, *S. aureus*), and culture-negative patients were entered into the study.

METHOD DETAILS

Sm Adhesion to human airway epithelia

A549 cells were cultured in 24-well plates (Thermo Fisher Scientific) ($2.0x10^5$ cells/well) and incubated for 24 h with increasing Sm inocula (MOI = $0.1\text{-}10^4$) or with Sm at MOI = 10^3 for increasing times (0–90 min) at 37°C in 5% CO_2. The cells were washed, fixed for 10 min with 2.5% glutaraldehyde, and washed again. Adherent bacteria were released with 0.05% trypsin and Sm CFUs enumerated after overnight incubation at 37°C on LB agar plates. In other experiments, Sm adhesion was measured using: 1) 1HAEo$^-$, CFTE29o$^-$, 16HBE14o$^-$, BEAS-2B, or A549 cells, SAECs, or a no cell control, incubated for 30 min at 37°C with Sm at MOI = 10^3, 2) A549 cells or SAECs were incubated for 30 min at 37°C with flagellin-expressing WT Sm or the flagellin-null Sm strain, both at MOI = 10^3, 3) A549 cells incubated for 30 min at 37°C with WT Sm at MOI = 10^3 in the presence of 0.25–25 μM of the Sm FliC1,2,3 flagellin mixture, 1.0–100 μM of rMUC1-ED-WT, or the PBS control, or co-incubated with 2.7–267 μM of C9-BA-DANA or the PBS control, 4) HEK293T cells transfected for 24 h for expression of the TLR5 or MUC1 proteins, or the pcDNA3.1 empty vector control, and incubated for 30 min at 37°C with Sm at MOI = 10^3, 5) HEK293T cells infected for 48 h at 37°C with Ad-GFP or Ad-MUC1 and incubated for 30 min at 37°C with Sm at MOI = 10^3, 6) A549 cells pre-incubated with 2.7 μM of MUC1-targeting, NEU1-targeting, or nontargeting control siRNAs and incubated for 30 min at 37°C with Sm at MOI = 10^3, and 7) uninfected A549 cells or A549 cells infected for 48 h at 37°C with Ad-GFP, Ad-NEU1, Ad-NEU1-G68V, or Ad-NEU3 (each at MOI = 100) and incubated for 30 min at 37°C with Sm at MOI = 10^3.

Sm Adhesion to plastics

For PVC, 0.5 cm sections of an endotracheal tube (7.0 mm inside diameter, 9.5 mm outside diameter, 5.5 cm^2 surface area) (Serfinity Medical, Cerritos CA) were cut using a sterile surgical scalpel. For PS, untreated 24-well culture plates were used (1.9 cm^2/well) (Thermo Fischer Scientific). The plastics were incubated for 30 min at 37°C with 2.0×10^8 CFU of flagellin-expressing WT Sm or the flagellin-null Sm strain, washed with PBS, pH 7.2, and adherent bacteria quantified by CFU counting.[20] In other experiments, PVC and PS plastics were incubated for 30 min at 37°C with 2.0×10^8 CFU of WT Sm in the presence of 1.0–100 μM rMUC1-ED-WT or PBS control, washed, and adherent bacteria quantified.

Purification of Sm flagellins

An overnight culture of WT Sm strain KJ was centrifuged at 5,000xg for 30 min at 4°C, resuspended in Krebs-Ringer buffer, and incubated for 1 h at 37°C. The bacteria were collected by centrifugation, and the supernatant was filtered through a 0.22 μm pore membrane (Millipore) and boiled for 20 min. The filtrate was concentrated by centrifugal ultrafiltration using membrane filters (pore size 10 kDa) mounted in Centricon tubes (Millipore), adjusted to pH 4.0 with 0.05 M sodium acetate buffer, and the Sm FliC1, FliC2, and FliC3 proteins purified by ion-exchange chromatography on a Macro-Prep High Q resin column (Bio-Rad). Two purification methods were used: 1) the Macro-Prep High Q resin was washed with 0.05 M sodium acetate buffer, pH 4.0, and the mixture of Sm FliC1, FliC2, and FliC3 proteins (FliC1,2,3) eluted as a single batch with 50 mM Bis-Tris buffer, pH 8.0 as monitored at A_{280} and 2) the Macro-Prep High Q resin was washed with 0.05 M sodium acetate buffer, pH 4.0, and the individual FliC1, FliC2, and FliC3 proteins eluted using a linear gradient of 50 mM Bis-Tris from pH 4.0 to 8.0. One mL fractions were collected, and A_{280} and pH of each fraction measured. The eluted FliC1,2,3 flagellin mixture and individual FliC1, FliC2, and FliC3 proteins were incubated for 1 h at 4°C with polymyxin B-agarose (Thermo Fisher Scientific) to remove lipopolysaccharide, after which less than 0.1 endotoxin units/μg of protein was detected by the *Limulus* amebocyte lysate assay.[22]

SDS-PAGE and immunoblot assays

Sm bacteria were concentrated by centrifugation at 5,000xg for 30 min at 4°C, washed with PBS, pH 7.2 at 4°C, the bacterial pellet sonicated on ice using a probe sonicator, and the sonicate centrifuged at 10,000xg for 15 min at 4°C.[93] A549 and HEK293T cells were rinsed with ice-cold HEPES buffer, lysed with 50 mM Tris-HCl, pH 8.0, 1.0% Nonidet P-40, 0.5% SDS, 150 mM NaCl, 0.1 mM phenylmethylsulfonyl fluoride, 5.0 μg/mL leupeptin, 1.0 mg/mL pepstatin A, 1.0 mg/mL aprotinin, 1.0 mM vanadate, 1.0 mM sodium fluoride, 10 mM disodium pyrophosphate, 500 μM *p*-nitrophenol, and 1.0 mM phenylarsine oxide, and the protein concentration using the Bio-Rad Protein Assay Dye Reagent. Equal amounts of protein were resuspended in Laemmli sample buffer containing 10% 2-mercaptoethanol, heated for 10 min at 95°C, and resolved by discontinuous polyacrylamide gel electrophoresis on 8–16% separating gels containing 25 mM Tris-HC1, 190 mM glycine, and 0.1% SDS, pH 8.3. Resolved proteins were stained overnight at 22°C with 0.1% Coomassie R-250 in 40% methanol and 10% acetic acid, and destained with 40% methanol and 10% acetic acid. For immunoblot analysis, resolved proteins in SDS-acrylamide gels were transferred to PVDF membranes and the membranes blocked for 1 h at 22°C using 5.0% nonfat milk in 50 mM Tris-HCl, pH 8.0, 150 mM NaCl, and 0.01% Tween 20 (TBS-T). The membranes were incubated for 1 h at 22°C with the appropriate primary Ab followed by incubation for 1 h at 22°C with the corresponding HRP-conjugated secondary Ab, and developed with ECL reagents. To confirm equivalent protein loading and transfer, the immunoblots were stripped with 62.5 mM Tris-HCl, pH 6.7, 100 mM 2-mercaptoethanol, and 2.0% SDS, washed with TBS-T, and reprobed with

mouse anti-β-tubulin Ab followed by HRP-conjugated goat anti-mouse Ab and developed with ECL reagents. For phospho(p)ERK1/2 immunoblots, the blots were stripped and reprobed for total ERK2.[42] For all blots, the bands of interest were quantified using ImageJ software (https://imagej.net/ij/).

Sm motility assay

Bacteria in mid-log phase (A_{600} = 0.5) were resuspended in LB medium, stab-inoculated into 0.3% LB agar plates, incubated overnight at 37°C, and colony diameters measured as an indicator of bacterial motility.[22] In other experiments, Sm were pre-incubated for 1 h at 37°C with 1.0–100 μM of rMUC1-ED-WT or the PBS control, washed, resuspended in LB medium, and analyzed for motility.

Fluorometric Sm flagellin binding assays

The FliC1,2,3 Sm flagellin mixture was labeled using the Alexa Fluor 594 conjugation kit (Abcam, Waltham, MA) according to the manufacturer's recommendations. A549 cells in 24-well plates ($2.0x10^5$ cells/well) were incubated for 30 min at 4°C with 10 nM of the Alexa Fluor 594-labeled FliC1,2,3 flagellin mixture in the presence of 0.1–10 nM of the unlabeled FliC1,2,3 flagellin mixture, the unlabeled individual FliC1, FliC2, or FliC3 flagellins, or PBS control. The cells were washed with PBS, pH 7.2 and bound flagellin determined by fluorometry (λex = 591 nm, λem = 615 nm).[21,22] In other experiments, A549 cells in 24-well plates were incubated for 30 min at 4°C with 10 nM of Alexa Fluor 594-labeled FliC1,2,3 in the presence of 0.01–100 nM of rMUC1-ED-WT, rMUC1-ED-Δ1, rMUC1-ED-Δ2, or PBS control, or with 1.0 μM of rMUC1-ED-Δ1, rMUC1-ED-Δ3, rMUC1-ED-Δ4, rMUC1-ED-Δ5 or PBS control. The cells were washed and bound flagellin determined. In still other experiments, A549 cells in 24-well plates were transfected for 48 h at 37°C in 5% CO_2 with 1.0 μg/well of the pcDNA3.1 plasmid incorporating the full-length MUC1 cDNA (pMUC1) or the pcDNA3.1 empty vector control, or with 2.7 μM of the MUC1-targeting or nontargeting control siRNAs, and washed with PBS, pH 7.2. The cells were incubated for 30 min at 4°C with 0.2–8.0 nM of the Alexa Fluor 594-labeled FliC1,2,3 flagellin mixture, washed again, and bound flagellin determined. Scatchard analysis of the binding data were performed to quantify the number of flagellin binding sites on the cells, as indicated by the X axis intercept of the binding plot, and the binding affinity of the flagellin-MUC1-ED interaction, as indicated by the slope of the binding plot ($-1/K_d$), where K_d represents the dissociation constant.[21,22] In yet other experiments, A549 cells in 24-well plates were infected for 48 h at 37°C with Ad-GFP, Ad-NEU1, Ad-NEU1-G68V, or Ad-NEU3 (each at MOI = 100) or transfected for 48 h at 37°C with 2.7 μM of NEU1-targeting or nontargeting control siRNAs. The cells were washed, incubated for 30 min at 4°C with 0.2–8.0 nM of the Alexa Fluor 594-labeled FliC1,2,3 flagellin mixture, washed again, bound flagellin was determined, and Scatchard analysis performed. Finally, A549 cells in 24-well plates were incubated for 30 min at 4°C with 0.2–8.0 nM of the Alexa Fluor 594-labeled FliC1,2,3 flagellin mixture in the presence of 100 μM rMUC1-ED, 267 μM (100 μg/mL) of C9-BA-DANA, or PBS control, washed again, bound flagellin determined, and Scatchard analysis performed.

Flagellin structural analyses

The X-ray crystal structures of the Pa FlaA and STm FliC flagellins, and the cryogenic electron microscopy (cryo-EM) structure of Pa FlaB have been reported.[94–96] In the absence of X-ray crystallographic or cryo-EM data, aa sequences of the 3 Sm flagellins[20] and single Lp flagellin (GenBank accession number ANN95373.1) were used to model their respective tertiary structures using AlphaFold2 and RoseTTAFold.[86,87] The 7 flagellin proteins (Sm FliC1, FliC2, and FliC3, Pa FlaA and FlaB, Lp FliC, and STm FliC) were superimposed over either their D0/D1 domains or their D2 domain β-sheets, and corresponding regions analyzed using UCSF ChimeraX.[88]

Adenoviral constructs

NEU1 (GenBank accession number NM_000434.3) and NEU3 (GenBank accession number NM_006656.5) sequences were synthesized by Primm Biotech (Cambridge, MA). A plasmid encoding the catalytically dead NEU1-G68V mutant was kindly provided by Dr. L. Debelle (Université de Reims, Reims, France). The NEU1, NEU1-G68V, and NEU3 sequences were subcloned into an Ad vector using the AdEasy Adenoviral Vector System (Stratagene, La Jolla, CA) according to the manufacturer's recommendation.[85] Briefly, each sequence was subcloned into the pShuttle-IREs-hrGFP-1 shuttle vector using appropriate restriction enzymes and ligation. Each resultant shuttle plasmids were linearized by *Pme*I digestion and, with the Ad backbone plasmid (pAdEasy-1, Qbiogene/MP Biomedicals, Solon, OH), were used to co-transform electrocompetent *E. coli* BJ5183 cells to produce recombinant plasmids. Recombinant plasmids were selected for kanamycin resistance and screened for recombination by *Pac*I digestion. Recombinant plasmids were used to transform XL10-Gold cells and bacterial lysates were passed through Maxiprep columns (Qiagen, Germantown, MD) for plasmid purification. Ad-NEU1, Ad-NEU1-G68V, and Ad-NEU3 were linearized by *Pac*I digestion and transfected in the presence of lipofectamine (Invitrogen) into AD-293 cells. After 7–10 days, cells were scraped off flasks with a rubber policeman and subjected to 3 freeze-thaw cycles, and virus was harvested in the supernatants for presentation to fresh AD-293 cells and titration in a plaque-forming assay. Ad-GFP and Ad-MUC1 were purchased from GenScript (Piscataway, NJ).

Manipulation of MUC1, TLR5, and NEU1 expression

To overexpress TLR5 or MUC1, A549 and HEK293T cells were transfected with plasmids encoding for TLR5 or MUC1, or the empty vector control (pcDNA3.1), and cultured for 48 h[21,22] To overexpress NEU1, A549 cells were infected with Ad-NEU1 or an Ad-GFP vector control.[21,22] As additional controls, cells were infected with Ad-NEU1-G68V or Ad-NEU3.[21,97] To silence MUC1 or NEU1 expression, cells were centrifuged, and the pellet was resuspended in 100 μL of Amaxa Nucleofector solution (Lonza) with 2.7 μg of MUC1-targeting or NEU1-targeting

siRNAs, or irrelevant control siRNA duplexes not corresponding to any known sequence in the human genome.[21,30,97] Each cell-siRNA mixture was transferred to an Amaxa-certified cuvette and subjected to programmed electroporation, and the transfected cells cultured for 72 h. To confirm protein overexpression and/or knockdown, the transfected or infected cells were lysed and the lysates processed for MUC1, TLR5, or NEU1 immunoblotting.

Expression and purification of human rMUC1-ED and its deletion mutants

The 375 aa full-length human MUC1-ED-WT cDNA in the pcDNA3.1 plasmid has been reported.[59] The rMUC1-ED deletion mutants containing 15 (rMUC1-ED-Δ1, aa 1–311), 6 (rMUC1-ED-Δ3, aa 1–131), 3 (rMUC1-ED-Δ4, aa 1–71), or 1 (rMUC1-ED-Δ5, aa 1–31) tandem repeat(s), and the rMUC1-ED deletion mutant containing only the SEA domain (MUC1-ED-Δ2, aa312-375), all in the pET-21b plasmid, were purchased from GenScript and subcloned into pBAD/His-B using standard procedures.[98] The 6XHis-tagged rMUC1-ED-WT, -Δ1, -Δ2, -Δ3, -Δ4, and -Δ5 plasmids were transformed into *E. coli* NEB 5-alpha competent cells (New England Biolabs, Ipswich, MA), the cells cultured to mid-log phase (A_{600} = 0.5), induced for 3 h at 37°C with 0.01% arabinose, and lysed by sonication. The 6X-His-tagged rMUC1-ED-WT, -Δ1, -Δ2, -Δ3, -Δ4, and -Δ5 proteins were purified on a Ni-NTA-agarose affinity column, and their purities confirmed on Coomassie blue-stained SDS-polyacrylamide gels.[22,23]

6XHis-rMUC1-ED protein binding assays

Equal protein aliquots of the purified Sm FliC1,2,3 flagellin mixture were incubated for 3 h at 4°C with the 6XHis-tagged MUC1-ED-WT, aa1-375, MUC1-ED-Δ1, aa1-311, or MUC1-ED-Δ2, aa312-375 proteins immobilized on Ni-NTA-agarose beads or with Ni-NTA-agarose beads alone.[99] The agarose-bound flagellin was eluted with PBS, pH 7.2 containing 300 mM imidazole and dialyzed against PBS, pH 7.2. The agarose-bound and unbound proteins were resolved by SDS-PAGE, transferred to PVDF membranes, and processed for flagellin immunoblotting.

MUC1-NEU1, MUC1-PPCA, and NEU1-MUC1 Co-Immunoprecipitation assays

A549 cells in 24-well plates ($2.0x10^5$ cells/well) were cultured for 1 h at 37°C in 5% CO_2 in the presence of Sm (MOI = 10^3) or the PBS vehicle control. The cells were washed with PBS, pH 7.2 and lysed with 50 mM Tris-HCl, pH 8.0, 1.0% Nonidet P-40, 150 mM NaCl, 0.1 mM phenylmethylsulfonyl fluoride, 5.0 μg/mL leupeptin, 1.0 mg/mL pepstatin A, 1.0 mg/mL aprotinin, 1.0 mM vanadate, 1.0 mM sodium fluoride, 10 mM disodium pyrophosphate, 500 μM *p*-nitrophenol, and 1.0 mM phenylarsine oxide, and the lysates centrifuged at 10,000xg for 15 min at 4°C and incubated overnight at 4°C with anti-MUC1-CD or anti-NEU1 Abs. The resultant immune complexes were immobilized by incubation with protein G agarose for 2 h at 4°C, centrifuged, washed, processed for immunoblotting with anti-NEU1, anti-MUC1-CD, or anti-PPCA Abs.[21–23,30] In other experiments, Ad-NEU1 infected A549 cells (MOI = 100) were co-incubated for 1 h at 37°C with Sm in the presence of 267 μM of C9-BA-DANA or the PBS control and lysed. To control for protein loading and transfer of immunoprecipitates, the blots were stripped and reprobed with the immunoprecipitating Ab. Each MUC1-CD signal was normalized to either the NEU1 or PPCA signal and each NEU1 signal was normalized to the MUC1-CD signal in the same lane in the same stripped and reprobed blot.

Fluorometric assay for sialidase activity

A549 cells ($1.0x10^6$ cells/reaction) were suspended in 200 μL of 500 mM sodium acetate, pH 4.4 containing 0.1% Triton X-100 and protease inhibitor mixture (Thermo Fisher Scientific) and co-incubated for 1 h at 37°C with 25 μL of 2.0 mM 4-MU-NANA and 2.7–267 μM of C9-BA-DANA or PBS control, mixing the tubes every 15min. The sialidase reaction was terminated by addition of 133 mM glycine, pH 10.3, 60 mM NaCl, and 0.083 M Na_2CO_3, after which the fluorescence intensity was measured with a Bio-Rad fluorometer (λex = 355 nm, λem = 460 nm).[30,43,85]

PNA lectin blotting of desialylated MUC1-ED

PNA lectin binds to subterminal galactose residues after removal of terminal sialic acid.[100] Asialofetuin (1.0 μ g) was used as a positive control for PNA-binding proteins and fetuin (1.0 μg) was used as a negative control. Equal protein aliquots of cell culture supernatants or total cell lysates, or mouse or human BALFs, were immunoprecipitated overnight at 4°C with anti-mouse MUC1-ED or anti-human MUC1-ED Abs, or incubated for 1 h at 4°C with PNA immobilized on agarose beads to selectively enrich for PNA-binding proteins.[21–23,30] The MUC1-ED immunoprecipitates and the PNA-bound protein were resolved by SDS-PAGE. Here, in order to adequately visualize the >250 kDa MUC1-ED protein, SDS-polyacrylamide discontinuous gel electrophoresis was performed under reducing condition in 3% stacking/5% separating acrylamide gels containing 25 mM Tris-HC1, 190 mM glycine, 0.1% SDS, pH 8.3 until the 150 kDa prestained protein MW marker reached the bottom of the gel.[21–23,30] The resolved proteins were transferred to PVDF membranes and the membranes incubated for 1 h at 22°C with either biotinylated PNA followed by incubation for 1 h at 22°C with HRP-conjugated streptavidin, or for 1 h at 22°C with anti-human or anti-mouse MUC1-ED Abs followed by incubation for 1 h at 22°C with HRP-conjugated secondary Abs, and ECL reagents. In the case of the MUC1-ED immunoprecipitates, to confirm equivalent protein loading and transfer, blots were stripped and reprobed with anti-MUC-ED Ab followed by HRP-conjugated secondary Ab and ECL reagents. For the human MUC1-ED desialylation experiments, the PNA and MUC1-ED signals for each of the PBS controls were set to 1.0 and the corresponding PBS-normalized PNA and MUC1-ED signals for the Sm-exposed cells calculated

MUC1-ED shedding by human airway epithelia, *in vitro*

A549 cells ($2.0x10^5$ cells/well) in 24-well plates were incubated for 24 h at 37°C in 5% CO_2 with increasing Sm inocula (MOI = 0.1-10^4 CFUs) or for increasing times (0–48 h) at 37°C in 5% CO_2 with Sm at MOI = 10^3 or the PBS control, and MUC1-ED levels in cell culture supernatants were measured by ELISA and normalized to total cell protein.[21–23] In other experiments, normalized MUC1-ED levels in cell culture supernatants were calculated in 1) 1HAEo$^-$, CFTE29o$^-$, 16HBE14o$^-$, BEAS-2B, A549 cells, SAECs, or a no cell control, incubated for 24 h at 37°C with Sm at MOI = 10^3, 2) A549 cells or SAECs incubated for 24 h at 37°C with flagellin-expressing WT or flagellin-null Sm, both at MOI = 10^3, 3) A549 cells incubated for 24 h at 37°C in 5% CO_2 with 0.25–25 μM of the purified FliC1,2,3 flagellin mixture, or with 25 μM of the purified individual FliC1, FliC2, or FliC3 flagellin proteins, 4) A549 cells pre-incubated for 48 h at 37°C with 2.7 μM of the NEU1-targeting or nontargeting control siRNAs, or with 267 μM of C9-BA-DANA or PBS control, and incubated for 24 h at 37°C with Sm at MOI = 10^3, and 5) HEK293T cells transfected for 24 h for expression of the full-length WT rMUC1 or rMUC1-S317A proteins and incubated for 24 h at 37°C with Sm at MOI = 10^3.

Detection of Sm-mouse/human MUC1-ED complexes

BALF from mice administered i.n. with 1.0×10^8 CFU/mouse of the flagellin-expressing WT Sm or flagellin-null Sm strains, and human BALF from patients with Sm lung infections or infections with other bacteria, were centrifuged at 10,000xg for 30 min at 4°C to pellet the bacteria, and the bacterial pellet washed with PBS, pH 7.2. The bacteria were resuspended in Laemmli SDS-PAGE sample buffer containing 10% 2-mercaptoethanol, heated for 10 min at 95°C, and processed for mouse or human MUC1-ED immunoblotting as above.

ELISAs for mouse and human MUC1-ED, and human IL-8

Mouse and human BALFs or human cell supernatants were centrifuged at 10,000xg for 10 min at 4°C, added in triplicate to 96-well ELISA plates (Thermo Fisher Scientific), and incubated overnight at 4°C. Wells were blocked for 1 h at 22°C with PBS, pH 7.2, containing 10 mg/mL bovine serum albumin, and 50 mg/mL sucrose, and washed with TBS-T. The samples were reacted for 2 h at 22°C with 200 μg/mL of rabbit anti-mouse or mouse anti-human MUC1-ED Ab, or mouse anti-human IL-8 Ab, washed with TBS-T, reacted for 2 h at 22°C with 200 μg/mL of HRP-conjugated goat anti-mouse IgG or HRP-conjugated goat anti-human IgG secondary Abs, and washed with PBS-T. Bound antibodies were detected with tetramethylbenzidine substrate at A_{450}.[23] Standard curves were generated using purified murine/human rMUC1-ED-WT and human rIL-8 proteins.

Sm biofilm assay

Overnight cultures of Sm in LB medium were adjusted to A_{600} = 0.1 in M9 medium, incubated for 48 h at 37°C in 96-well tissue culture plates (Thermo Fisher Scientific) with 1.0–100 μM of rMUC1-ED-WT, or the PBS control, washed with deionized water, stained with 0.1% crystal violet for 10 min at 22°C, and washed with deionized water. The crystal violet was solubilized with 30% acetic acid for 10 min at 22°C and A_{595} measured.[22,23]

QUANTIFICATION AND STATISTICAL ANALYSIS

All values were expressed as mean ± SEM. Power and sample size analyses were performed, as described.[101,102] Values for n are indicated in each figure and figure legend. Two sample comparisons were performed by the two-tailed Student's t test using the Microsoft Excel Analysis ToolPak add-in (Microsoft, Redmond, WA). Multiple sample comparisons were performed by analysis of variance (ANOVA) with Duncan's multiple range test using SAS software (version 9.4, SAS Institute, Cary, NC). For Scatchard analysis of fluorometric Sm flagellin binding data, linear trendlines, the corresponding linear regression equations, and R^2 values were calculated using Microsoft Excel. Kaplan-Meier survival curves of Pa-infected mice were compared using the Mantel-Cox log rank test (https://www.evanmiller.org/ab-testing/survival-curves.html). Statistical significance was set at $p < 0.05$.